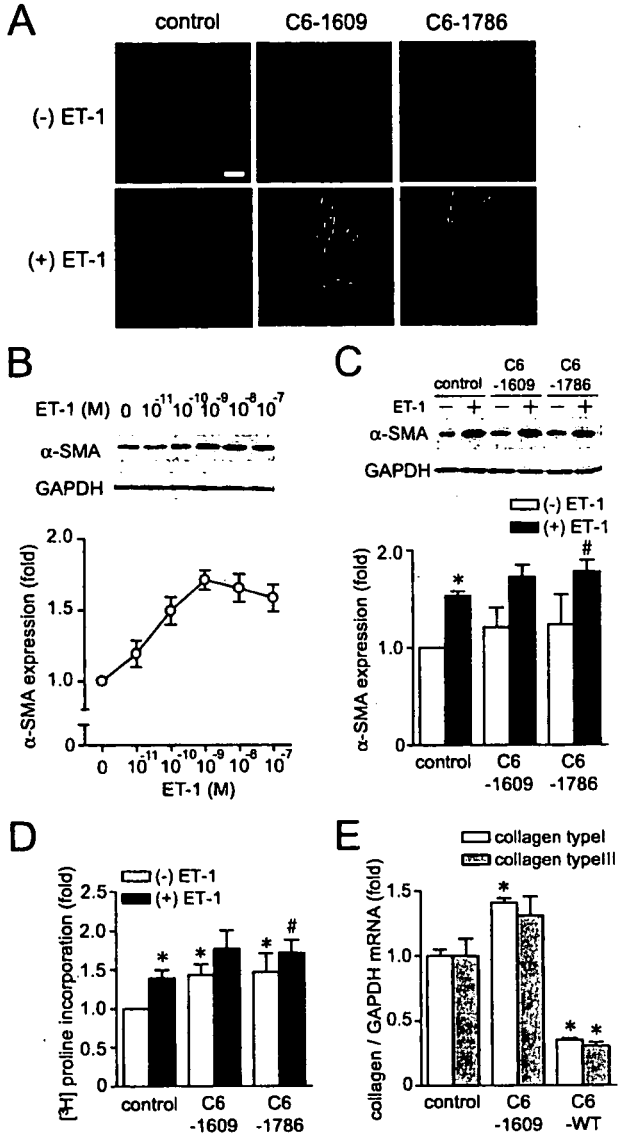

FIGURE 6. **Knockdown of TRPC6 enhances cardiac myofibroblast formation.** *A–C*, effects of TRPC6 siRNAs on the ET-1-induced increase in α-SMA expression. Forty-eight h after transfection with siRNAs, cells were treated with ET-1 (100 nM) for 24 h. *A*, immunohistochemistry of cardiac fibroblasts stained with anti-α-SMA antibody. *Scale bar*, 20 μm. *B* and *C*, concentration-dependent increase in α-SMA expression by ET-1 treatment (*B*) and changes in α-SMA expression by TRPC6 knockdown (*C*) were determined by Western blotting. *D*, effects of TRPC6 siRNAs on [^{3}H]proline incorporation in cardiac fibroblasts with or without ET-1 treatment. *E*, effects of TRPC6 siRNA and WT TRPC6 on the mRNA expression of collagen type I and III. *, $p < 0.05$ *versus* nontreatment (no ET-1) of control cells. #, $p < 0.05$ *versus* ET-1 treatment of control cells.

pathway plays a critical role in the pathogenesis of heart failure, we examined whether TRPC6-mediated NFAT activation participates in ET-1 treatment-induced transformation of cardiac fibroblasts. Treatment with ET-1 increased α-SMA expression in a concentration-dependent manner (Fig. 6, *A* and *B*). Treatment with ET-1 (1 nM) caused maximal α-SMA expression, whereas ET-1 treatment (>10 nM) slightly decreased α-SMA expression. Knockdown of TRPC6 did not affect basal α-SMA protein expression levels. However, it weakly but significantly enhanced ET-1-induced α-SMA expression (Fig. 6, *A* and *C*). Furthermore, TRPC6 siRNAs significantly enhanced the basal incorporation of [^{3}H]proline, an index of synthesis of ECM proteins (Fig. 6*D*). TRPC6 siRNAs also enhanced ET-1-induced [^{3}H]proline incorporation. Collagen expression is another index of transformation of cardiac fibroblasts to myofibroblasts. TRPC6 siRNA increased mRNAs of collagen type I and III, whereas overexpression of WT TRPC6 significantly suppressed the basal expression of collagen mRNAs (Fig. 6*E*). These results suggest that TRPC6 negatively regulates ET-1-induced transformation of cardiac fibroblasts to myofibroblasts and synthesis of ECM components.

Inhibition of Cardiac Myofibroblast Formation by NFAT Activation—The expression of TRPC6 WT inhibited the collagen mRNA expression and enhanced NFAT activation by ET-1 treatment (Figs. 5*G* and 6*E*). In addition to cardiac fibroblasts, we have previously demonstrated in cardiac myocytes that TRPC6 regulates NFAT activation (12). Then we examined whether TRPC6-mediated NFAT activation negatively regulates ET-1-induced transformation of cardiac fibroblasts to myofibroblasts. The expression of CA NFAT increased basal NFAT activity (8.3 ± 0.9-fold) and suppressed the increase in α-SMA expression by ET-1 treatment (Fig. 7, *A* and *B*). Expression of α-SMA by ET-1 treatment was also suppressed by expression of TRPC6 WT. In contrast, treatment with CysA increased the basal α-SMA expression levels and [^{3}H]proline incorporation, which was further enhanced by ET-1 treatment (Fig. 7, *B* and *D*). These results suggest that TRPC6-mediated NFAT activation inhibits ET1-induced α-SMA expression in cardiac fibroblasts. Furthermore, the ET-1-induced increase in α-SMA expression and [^{3}H]proline incorporation was suppressed by the expression of p115-RGS and DN Rac and treatment with SP600125 (Fig. 7, *C* and *D*). These results suggest that the $G\alpha_{12/13}$-mediated signaling pathway ($G\alpha_{12/13}$-Rac-JNK) mediates ET-1-induced myofibroblast formation in cardiac fibroblasts. However, $G\alpha_{12/13}$-mediated NFAT activation negatively regulates ET-1-induced cardiac myofibroblast formation.

Inhibition of ET-1-induced JNK Activation by TRPC6-mediated NFAT Activation—In order to examine how NFAT attenuates myofibroblast formation by ET-1 treatment, we next examined the effects of NFAT on ET-1-induced mitogen-activated protein kinase activation. Treatment with ET-1 increased JNK activity, which was suppressed by the expression of CA NFAT and WT TRPC6 but was potentiated by CysA (Fig. 8*A*). However, the ET-1-induced ERK activation was not affected by CA NFAT, TRPC6 WT, and CysA (Fig. 8*B*). This is consistent with the result that ERK activation is not involved in the increased expression of TRPC6 by ET-1 treatment (supplemental Fig. 2*C*). These results suggest that NFAT activation through TRPC6 up-regulation specifically inhibits ET-1-induced JNK activation in cardiac fibroblasts. The ET-1-induced ROS production and Rac activation, both of which work upstream of JNK, were suppressed by TRPC6 overexpression and NFAT activation (Fig. 8, *C* and *D*). These results suggest that NFAT inhibits JNK activation through inhibition of Rac activation and ROS production.

Requirement of TRPC6 Up-regulation in ET-1-induced Hypertrophic Responses of Cardiomyocytes—It has been reported that up-regulation of TRPC6 amplifies calcineurin

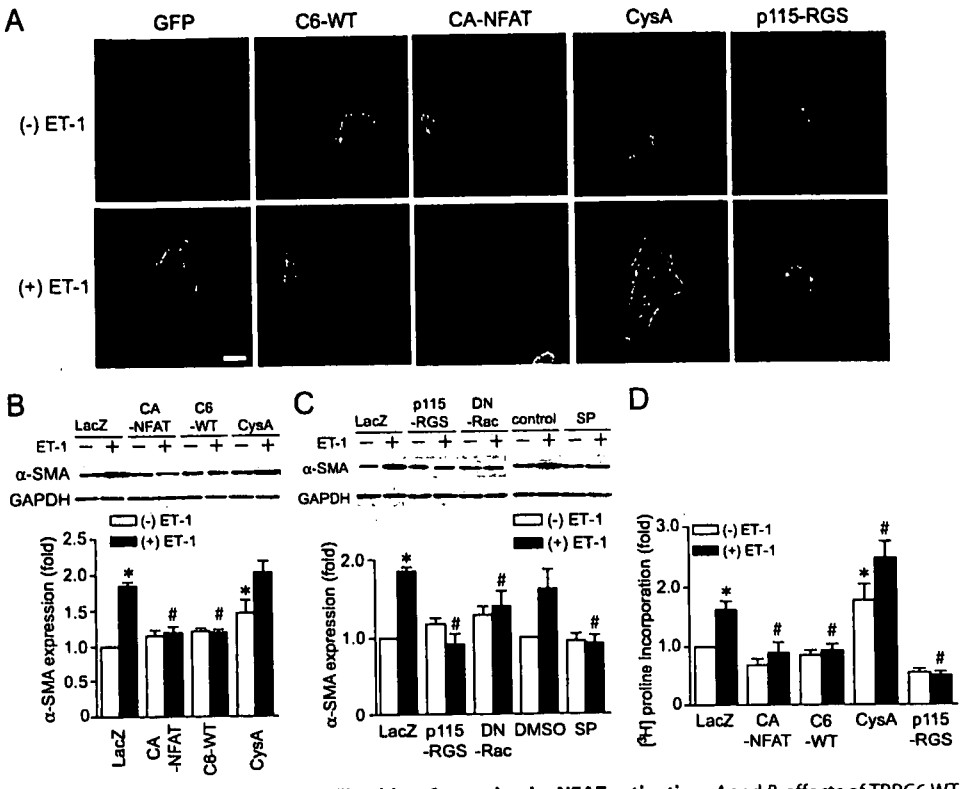

FIGURE 7. **Inhibition of cardiac myofibroblast formation by NFAT activation.** *A* and *B*, effects of TRPC6 WT, CA NFAT, CysA, and p115-RGS on the ET-1-induced increase in α-SMA expression. Cells were infected with adenovirus coding one of TRPC6 WT, p115-RGS, and CA NFAT at a multiplicity of infection of 100 for 24 h and then treated with ET-1 (100 nM) for 48 h. Cells were treated with CysA (0.5 μg/ml) for 20 min prior to ET-1 treatment. *A*, immunohistochemistry of cardiac fibroblasts stained with anti-α-SMA antibody. *Scale bar*, 20 μm. *B*, changes in α-SMA expression determined by Western blotting. *C*, effects of p115-RGS, DN Rac, and SP600125 on the ET-1-induced increase in α-SMA expression. Twenty-four h after infection with adenovirus coding one of LacZ, p115-RGS, and DN Rac, cells were treated with ET-1 for 48 h. Cells were treated with SP600125 (*SP*; 1 μM) for 20 min prior to ET-1 treatment. *D*, effects of CA NFAT, TRPC6 WT, CysA, and p115-RGS on [^{3}H]proline incorporation in cardiac fibroblasts with or without ET-1 treatment. *, $p < 0.05$ *versus* nontreatment (no ET-1) of LacZ-expressing cells. #, $p < 0.05$ *versus* ET-1 treatment of LacZ-expressing cells.

signaling, leading to pathologic cardiac remodeling in mice (37). We have previously reported that $G\alpha_{12/13}$-mediated JNK activation participates in ET-1-induced hypertrophic responses of cardiomyocytes (24). We examined whether TRPC6 up-regulation is involved in ET-1-induced hypertrophic growth of rat neonatal cardiomyocytes. Treatment with ET-1 increased TRPC6 protein levels in a concentration-dependent manner, and the EC_{50} value was about 3 nM (Fig. 9*A*). The ET-1-induced increase in TRPC6 protein expression was completely suppressed by p115-RGS (Fig. 9*B*), suggesting that $G\alpha_{12/13}$ mediate ET-1-induced TRPC6 up-regulation. Treatment with ET-1 increased BNP-luciferase activity, a marker for cardiac hypertrophy, and the EC_{50} value was about 5 nM (Fig. 9*C*). ET-1-stimulated BNP-luciferase activity was blocked by expression of p115-RGS, an inhibitory polypeptide of $G\alpha_{12/13}$. This result suggests that $G\alpha_{12/13}$ mediate ET-1-stimulated hypertrophic response. Although we could not reliably determine the effects of TRPC6 siRNAs on ET-1-stimulated BNP-luciferase activity, the ET-1-induced NFAT activation and hypertrophic responses (actin reorganization and protein synthesis) were significantly suppressed by TRPC6 siRNAs (Fig. 9, *D–F*). These results suggest that $G\alpha_{12/13}$ also play a role in ET-1-induced increase in TRPC6 protein expression in cardiomyocytes. However, in the case of cardiomyocytes, the up-regulated TRPC6 may positively regulate hypertrophic responses induced by ET-1.

DISCUSSION

In this study, we demonstrated that TRPC6 proteins are up-regulated by ET-1 treatment in cardiac fibroblasts. Furthermore, we demonstrated that the ET-1-induced increase in TRPC6 expression is critical for NFAT activation, which negatively regulates myofibroblast formation. Previous reports have shown that TRPC6 proteins are up-regulated by ET-1 and platelet-derived growth factor in pulmonary vascular smooth muscle cells (34, 35). These reports are consistent with the present results. We first demonstrated that $G\alpha_{12/13}$ mediate ET-1-induced up-regulation of TRPC6 mRNAs and proteins in cardiac fibroblasts. We previously reported that $G\alpha_{12/13}$ mediate Ang II-induced JNK activation through Rac-dependent ROS production (17, 25). Since it was reported that c-Jun, one of the target molecules of JNK, is required for agonist-induced up-regulation of TRPC6 proteins in pulmonary vascular smooth muscle cells (36), $G\alpha_{12/13}$-mediated JNK activation may participate in the increased expression of TRPC6 in cardiac fibroblasts. Furthermore, we clearly demonstrated that $G\alpha_{12/13}$ mediate ET-1-induced myofibroblast formation, since p115-RGS completely suppressed the increase in α-SMA expression and [^{3}H]proline incorporation by ET-1 treatment (Fig. 6). Since ET-1-induced myofibroblast formation was also suppressed by DN Rac and SP600125 (Fig. 6*C*), the $G\alpha_{12/13}$-Rac-JNK signaling pathway may be involved in ET-1-induced myofibroblast formation. However, ET-1-induced fibrotic responses were inhibited by up-regulation of TRPC6 expression and resultant NFAT activation through the $G\alpha_{12/13}$-mediated pathway (Fig. 6). Therefore, ET-1 treatment caused fibrotic responses through the Rac-JNK pathway, and at the same time ET-1 treatment negatively regulated fibrotic responses through NFAT activation by the increased expression of TRPC (Fig. 10). The concentration of ET-1 to induce maximal α-SMA expression was about 1 nM, which was about 10 times lower than that of ET-1 to induce maximal expression of TRPC6 proteins (Figs. 3*B* and 6*B*). Thus, cardiac fibroblasts may turn on their own protective system against excess progression of fibrotic responses when the cells are exposed to a high concentration of ET-1.

Although we cannot explain in detail the mechanism of how NFAT inhibits JNK activation (Fig. 8*A*) and TRPC6 expression

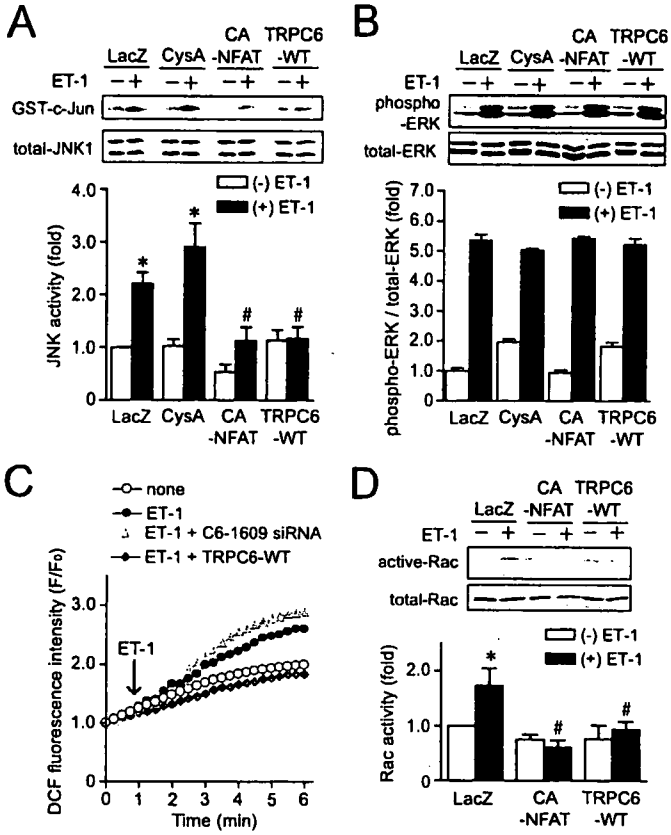

FIGURE 8. **Inhibition of ET-1-induced Rac activation, ROS production, and JNK activation by TRPC6-mediated NFAT activation.** *A* and *B*, effects of CA NFAT, CysA, and TRPC6 WT on ET-induced JNK activation (*A*) and ERK activation (*B*). Forty-eight h after infection with adenovirus coding one of LacZ, CA NFAT, and TRPC6 WT or 24 h after treatment with CysA (0.5 μg/ml), cells were treated with ET-1 (100 nM) for 20 min. *C*, effects of TRPC6 WT and TRPC6 siRNA (1609) on ET-1-induced ROS production. *D*, effects of CA NFAT and TRPC6 WT on ET-1-induced Rac activation. Cells were treated with ET-1 (100 nM) for 2 min. *, $p < 0.05$ *versus* nontreatment (no ET-1) of control or LacZ-expressing cells. #, $p < 0.05$ *versus* ET-1 treatment of control or LacZ-expressing cells.

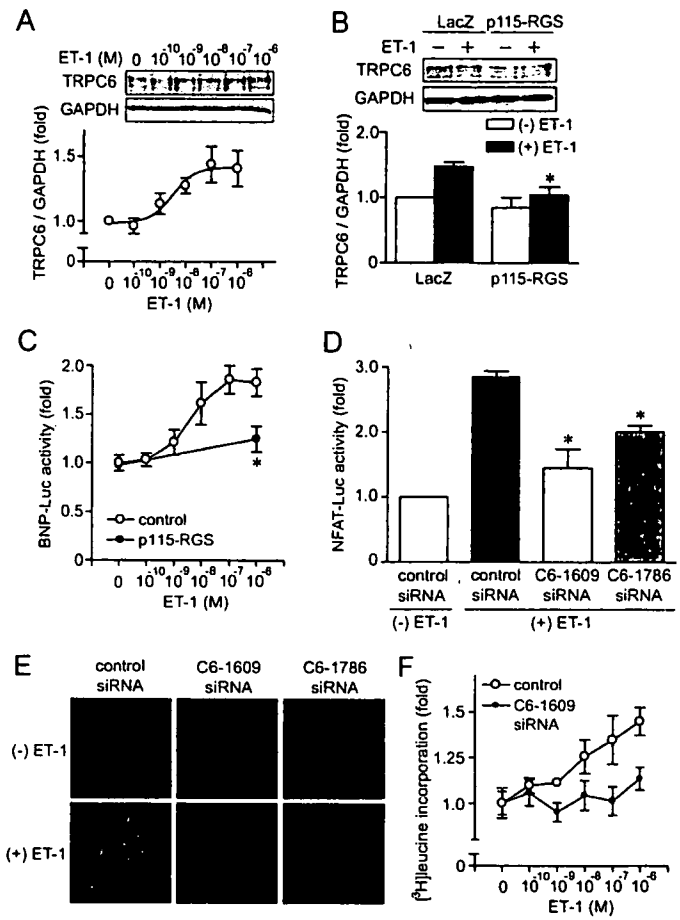

FIGURE 9. **Involvement of TRPC6 up-regulation in ET-1-induced hypertrophic responses of cardiomyocytes.** *A*, concentration-dependent increase in TRPC6 protein expression by ET-1 stimulation. Cells were treated with ET-1 for 48 h. TRPC6 proteins were detected with Western blot. *B*, effects of p115-RGS on ET-1-induced increase in TRPC6 protein expression. Twenty-four h after infection, cells were treated with ET-1 (100 nM) for 48 h. *C*, concentration-dependent increase in BNP-luciferase activity by ET-1 stimulation. Cells were treated with ET-1 for 24 h, and luciferase activity was determined. *D–F*, effects of TRPC6 siRNAs on ET-1-induced NFAT activation (*D*), actin reorganization (*E*), and protein synthesis (*F*). Forty-eight h after transfection with siRNAs, cells were treated with ET-1 for 24 h (*B* and *C*) or 8 h (*D*). *, $p < 0.05$ *versus* ET-1 treatment of control or LacZ-expressing cells.

(supplemental Fig. 2) induced by ET-1 stimulation, there are a couple of possibilities. Since DPI and SP600125 suppressed TRPC6 promoter activity by ET-1 treatment, the ROS-JNK pathway plays an important role in TRPC6 expression (Fig. 3*E*). Expression of CA NFAT suppressed ET-1-stimulated Rac activation, and we previously reported that Rac mediates JNK activation (17, 25). Therefore, NFAT inhibits TRPC6 expression through inhibition of the Rac-JNK pathway. We can exclude down-regulation of ET receptors as a mechanism of NFAT-mediated inhibition of TRPC6 expression, since the ET-1-induced ERK activation was not affected by CA NFAT and TRPC6 WT (Fig. 8*B*). Since NFAT acts as a transcriptional factor, one possibility is that some factor(s) produced by NFAT activation negatively regulates JNK activity through inhibition of Rac activation in cardiac fibroblasts. For example, NFAT is reported to regulate the expression levels of BMP2 (bone morphogenetic protein 2), an antifibrotic factor (38). Further studies are required for understanding the mechanism of NFAT-dependent inhibition of JNK activation.

It has been reported that TRPC6 channel activity is positively regulated by various stimuli, such as DAG (28), tyrosine phosphorylation (29), and mechanical stress (39). We found that the increase in $[Ca^{2+}]_i$ of CA $G\alpha_{13}$-expressing cells was completely inhibited by PP2 but not by U73122 (Fig. 2*D*), suggesting that Src tyrosine kinase but not PLC-generated DAG is involved in CA $G\alpha_{13}$-mediated Ca^{2+} influx. It also suggests that CA $G\alpha_{13}$ does not activate PLC in cardiac fibroblasts. We also found that AG1478 inhibits CA $G\alpha_{13}$-induced Src activation (Fig. 2*F*), suggesting the involvement of EGFR kinase in $G\alpha_{13}$-mediated Src activation. Our results suggest that CA $G\alpha_{13}$-mediated Src activation is involved in CA $G\alpha_{13}$-induced Ca^{2+} influx.

We also demonstrated that Ca^{2+} influx-induced increase in $[Ca^{2+}]_i$ evoked by ionomycin is not enhanced by TRPC6 overexpression (Fig. 4*C*). This result suggests that TRPC6 does not participate in store-operated Ca^{2+} entry in cardiac fibroblasts. TRPC1 is often referred to as a SOC, but it is unknown whether TRPC1 works as a true SOC, because this can also be activated by DAG and membrane stretch (19, 40). In addition to TRPC1, it has been recently reported that STIM1, located predominantly in the endoplasmic reticulum, acts as a Ca^{2+} sensor for store-operated Ca^{2+} entry (41, 42) and that Orai1/CRACM1 is identified as the Ca^{2+} release-activated Ca^{2+} channel gene (43,

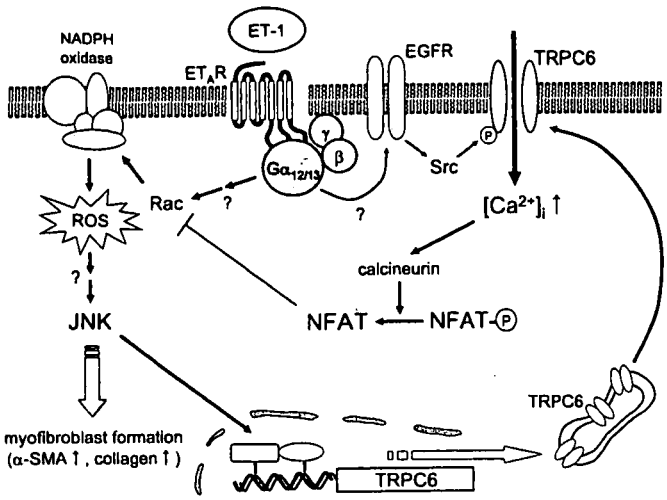

FIGURE 10. **Scheme for two opposite roles of $G\alpha_{12/13}$ in cardiac fibroblasts.** Stimulation of ET_AR by ET-1 treatment activates $G\alpha_{12/13}$, which mediate ET-1-induced TRPC6 up-regulation and myofibroblast formation through Rac-dependent ROS production and JNK activation. On the other hand, $G\alpha_{12/13}$-mediated Ca^{2+} influx through Src-dependent activation of up-regulated TRPC6 induces NFAT activation. The activated NFAT inhibits ET-1-induced Rac activation, ROS production, and JNK activation through unknown mechanism(s). NFAT may work as a negative feedback regulator against ET-1-induced myofibroblast formation in cardiac fibroblasts.

44). Since TRPC1, STIM1, and Orai1/CRACM1 are ubiquitously expressed, these molecules may participate in store-operated Ca^{2+} entry in cardiac fibroblasts.

A variety of evidence has implicated that the sustained increase in $[Ca^{2+}]_i$ is involved in the pathogenesis of heart failure (45). For example, up-regulation of TRPC proteins are associated with the reduction of sarcoplasmic reticulum Ca^{2+}-ATPase (20), suggesting the importance of TRPC in remodeling of the Ca^{2+} signaling mechanism in cardiac myocytes. Furthermore, it has been recently reported that diverse signals for cardiac hypertrophy stimulate the expression of TRPC channels and increase NFAT activity (21). Other groups demonstrated that the cardiac myocytes-specific expression of TRPC6 or CA calcineurin (upstream activator of NFAT) induces cardiac hypertrophy, and NFAT is activated in pathological but not physiological hypertrophy (46–48). We found in this study that $G\alpha_{12/13}$-mediated up-regulation of TRPC6 protein participates in ET-1-induced cardiomyocyte hypertrophy (Fig. 9). Thus, the TRPC-NFAT signaling pathway in myocytes plays an essential role in cardiac hypertrophy. In contrast to cardiac myocytes, we demonstrated in cardiac fibroblasts that up-regulation of TRPC6 expression and resultant activation of NFAT inhibit myofibroblast formation and synthesis of ECM components induced by ET-1 treatment. Therefore, we suggest that TRPC6 and TRPC6-mediated NFAT activation in cardiac fibroblasts work as negative regulators against cardiac fibrosis. Many lines of evidence have indicated that TRPC channels represent novel pharmacologic targets, since NFAT is activated by Ca^{2+} influx though TRPC channels in pathological hypertrophy. However, the role of TRPC channels in cardiac fibroblasts and cardiac fibrosis does not support this idea, since the TRPC6-NFAT signaling pathway works as a negative regulator of fibrotic responses. Inhibitor of TRPC channels may worsen the fibrotic process accompanied with hypertrophy. Since cardiac fibrosis leads to myocardial stiffness and diastolic dysfunction, future *in vivo* work will be required for understanding the role of TRPC proteins in the cardiac function and development of cardiac fibrosis. The present findings also indicate that activators of TRPC channel-NFAT signaling or downstream signaling components are novel anti-fibrotic drugs.

In summary, we have demonstrated a signal transduction pathway of ET-1-induced up-regulation of TRPC6 expression and NFAT activation. As the sustained increase in $[Ca^{2+}]_i$ through TRPC6 activates NFAT, the $G\alpha_{12/13}$-mediated TRPC6 expression and NFAT activation may act as a negative feedback regulator against ET-1-mediated fibrotic responses.

Acknowledgments—We thank Yuichi Nagamatsu for real time RT-PCR measurement during the early stage of this study and Yusuke Narita for production of CA NFAT adenovirus.

REFERENCES

1. Cohn, J. N., Ferrari, R., and Sharpe, N. (2000) *J. Am. Coll. Cardiol.* **35,** 569–582
2. Manabe, I., Shindo, T., and Nagai, R. (2002) *Circ. Res.* **91,** 1103–1113
3. Brown, R. D., Ambler, S. K., Mitchell, M. D., and Long, C. S. (2005) *Annu. Rev. Pharmacol. Toxicol.* **45,** 657–687
4. Braudino, T. A., Carver, W., Giles, W., and Borg, T. K. (2006) *Am. J. Physiol.* **291,** H1015–H1026
5. Tomasek, J. J., Gabbiani, G., Hinz, B., Chaponnier, C., and Brown, R. A. (2002) *Nat. Rev. Mol. Cell Biol.* **3,** 349–363
6. Swaney, J. S., Roth, D. M., Olson, E. R., Naugle, J. E., Meszaros, J. G., and Insel, P. A. (2005) *Proc. Natl. Acad. Sci. U. S. A.* **102,** 437–442
7. Powell, D. W., Mifflin, R. C., Valentich, J. D., Crowe, S. E., Saada, J. I., and West, A. B. (1999) *Am. J. Physiol.* **277,** C1–C9
8. Serini, G., and Gabbiani, G. (1999) *Exp. Cell Res.* **250,** 273–283
9. Kawano, H., Do, Y. S., Kawano, Y., Starnes, V., Barr, M., Law, R. E., and Hsueh, W. A. (2000) *Circulation* **101,** 1130–1137
10. Katwa, L. C. (2003) *Am. J. Physiol.* **285,** H1132–H1139
11. Wilkins, B. J., and Molkentin, J. D. (2004) *Biochem. Biophys. Res. Commun.* **322,** 1178–1191
12. Onohara, N., Nishida, M., Inoue, R., Kobayashi, H., Sumimoto, H., Sato, Y., Mori, Y., Nagao, T., and Kurose, H. (2006) *EMBO J.* **25,** 5305–5316
13. Shimoyama, M., Hayashi, D., Takimoto, E., Zou, Y., Oka, T., Uozumi, H., Kudoh, S., Shibasaki, F., Yazaki, Y., Nagai, R., and Komuro, I. (1999) *Circulation* **100,** 2449–2454
14. Øie, E., Bjørnerheim, R., Clausen, O. P. F., and Attramadal, H. (2000) *Am. J. Physiol.* **278,** H2115–H2123
15. Kolar, F., Papousek, F., MacNaughton, C., Pelouch, V., Milerova, M., and Korecky, B. (1996) *Mol. Cell Biochem.* **163,** 253–260
16. Yang, G., Meguro, T., Hong, C., Asai, K., Takagi, G., Karoor, V. L., Sadoshima, J., Vatner, D. E., Bishop, S. P., and Vatner, S. F. (2001) *J. Mol. Cell Cardiol.* **33,** 1505–1514
17. Fujii, T., Onohara, N., Maruyama, Y., Tanabe, S., Kobayashi, H., Fukutomi, M., Nagamatsu, Y., Nishihara, N., Inoue, R., Sumimoto, H., Shibasaki, F., Nagao, T., Nishida, M., and Kurose, H. (2005) *J. Biol. Chem.* **280,** 23041–23047
18. Nagamatsu, Y., Nishida, M., Onohara, N., Fukutomi, M., Maruyama, Y., Kobayashi, H., Sato, Y., and Kurose, H. (2006) *J. Pharmacol. Sci.* **101,** 144–150
19. Clapham, D. E. (2003) *Nature* **426,** 517–524
20. Seth, M., Sumbilla, C., Mullen, S. P., Lewis, D., Klein, M. G., Hussain, A., Soboloff, J., Gill, D. L., and Inesi, G. (2004) *Proc. Natl. Acad. Sci. U. S. A.* **101,** 16683–16688
21. Bush, E. W., Hood, D. B., Papst, P. J., Chapo, J. A., Minobe, W., Bristow, M. R., Olson, E. N., and McKinsey, T. A. (2006) *J. Biol. Chem.* **281,** 33487–33496
22. Nishida, M., Maruyama, Y., Tanaka, R., Kontani, K., Nagao, T., and Ku-

rose, H. (2000) *Nature* **408**, 492–495
23. Maruyama, Y., Nishida, M., Sugimoto, Y., Tanabe, S., Turner, J. H., Kozasa, T., Wada, T., Nagao, T., and Kurose, H. (2002) *Circ. Res.* **91**, 961–969
24. Arai, K., Maruyama, Y., Nishida, M., Tanabe, S., Takagahara, S., Kozasa, T., Mori, Y., Nagao, T., and Kurose, H. (2003) *Mol. Pharmacol.* **63**, 478–488
25. Nishida, M., Tanabe, S., Maruyama, Y., Mangmool, S., Urayama, K., Nagamatsu, Y., Takagahara, S., Turner, J. H., Kozasa, T., Kobayashi, H., Sato, Y., Kawanishi, T., Inoue, R., Nagao, T., and Kurose, H. (2005) *J. Biol. Chem.* **280**, 18434–18441
26. Inoue, R., Jensen, L. J., Shi, J., Morita, H., Nishida, M., Honda, A., and Ito, Y. (2006) *Circ. Res.* **99**, 119–131
27. Nishida, M., Sugimoto, K., Hara, Y., Mori, E., Morii, T., Kurosaki, T., and Mori, Y. (2003) *EMBO J.* **22**, 4677–4688
28. Hofmann, T., Obukhov, A. G., Schaefer, M., Harteneck, C., Gudermann, T., and Schultz, G. (1999) *Nature* **397**, 259–263
29. Hisatsune, C., Kuroda, Y., Nakamura, K., Inoue, T., Nakamura, T., Michikawa, T., Mizutani, A., and Mikoshiba, K. (2004) *J. Biol. Chem.* **279**, 18887–18894
30. Shi, C.-S., Sinnarajah, S., Cho, H., Kozasa, T., and Kehrl, J. H. (2000) *J. Biol. Chem.* **274**, 24470–24476
31. Kim, M., Nozu, F., Kusama, K., and Imawari, M. (2006) *Biochem. Biophys. Res. Commun.* **339**, 271–276
32. Lopez, I., Mak, E. C., Ding, J., Hamm, H. E., and Lomasney, J. W. (2001) *J. Biol. Chem.* **276**, 2758–2765
33. Gohla, A., Harhammer, R., and Schultz, G. (1998) *J. Biol. Chem.* **273**, 4653–4659
34. Yu, Y., Sweeney, M., Zhang, S., Platoshyn, O., Landsberg, J., Rothman, A., and Yuan, J. X-J. (2003) *Am. J. Physiol.* **284**, C316–C330
35. Kunichika, N., Landsberg, J. W., Yu, Y., Kunichika, H., Thistlethwaite, P. A., Rubin, L. J., and Yuan, J. X. (2004) *Am. J. Respir. Crit. Care. Med.* **170**, 1101–1107
36. Dietrich, A., Mederos y Schnizler, M., Gollasch, M., Gross, V., Storch, U., Dubrovska, G., Obst, M., Yildirim, E., Salanova, B., Kalwa, H., Essin, K., Pinkenburg, O. C., Luft, F., Gudermann, T., and Birnbaumer, L. (2005) *Mol. Cell Biol.* **25**, 6980–6989
37. Kuwahara, K., Wang, Y., McAnally, J., Richardson, J. A., Bassel-Duby, R., Hill, J. A., and Olson, E. N. (2006) *J. Clin. Invest.* **116**, 3114–3126
38. Koga, T., Matus, Y., Asagiri, M., Kodama, T., de Crombrugghe, B., Nakashima, K., and Takayanagi, H. (2005) *Nat. Med.* **11**, 880–885
39. Spassova, M. A., Hewavitharana, T., Xu, W., Soboloff, J., and Gill, D. L. (2006) *Proc. Natl. Acad. Sci. U. S. A.* **103**, 16586–16591
40. Lewis, R. S. (2007) *Nature* **446**, 284–287
41. Liou, J., Kim, M. L., Heo, W. D., Jones, J. T., Myers, J. W., Ferrell, J. E. Jr., and Meyer, T. (2005) *Curr. Biol.* **15**, 1235–1241
42. Roos, J., DiGregorio, P. J., Yeromin, A. V., Ohlsen, K., Lioudyno, M., Zhang, S., Safrina, O., Kozak, J. A., Wagner, S. L., Cahalan, M. D., Velicelebi, G., and Stauderman, K. A. (2005) *J. Cell Biol.* **169**, 435–445
43. Feske, S., Gwack, Y., Prakriya, M., Srikanth, S., Puppel, S. H., Tanasa, B., Hogan, P. G., Lewis, R. S., Daly, M., and Rao, A. (2006) *Nature* **441**, 179–185
44. Vig, M., Peinelt, C., Beck, A., Koomoa, D. L., Rabah, D., Koblan-Huberson, M., Kraft, S., Turner, H., Fleig, A., Penner, R., and Kinet, J. P. (2006) *Science* **312**, 1220–1223
45. Molkentin, J. D., Lu, J.-R., Antos, C. L., Markham, B., Richardson, J., Robbins, J., Grant, S. R., and Olson, E. N. (1998) *Cell* **93**, 215–228
46. Nakayama, H., Wilkin, B. J., Bodi, I., and Molkentin, J. D. (2006) *FASEB J.* **20**, 1660–1670
47. Wilkins, B. J., Dai, Y.-S., Bueno, O. F., Parsons, S. A., Xu, J., Plank, D. M., Jones, F., Kimball, T. R., Jeffery, D., and Molkentin, J. D. (2004) *Circ. Res.* **94**, 110–118
48. Frey, N., McKinsey, T. A., and Olson, E. N. (2000) *Nat. Med.* **6**, 1221–1227

Journal of Cellular Physiology

Granulocyte Colony-Stimulating Factor Promotes the Translocation of Protein Kinase Cι in Neutrophilic Differentiation Cells

TOSHIE KANAYASU-TOYODA,[1] TAKAYOSHI SUZUKI,[1] TADASHI OSHIZAWA,[1] ERIKO UCHIDA,[2] TAKAO HAYAKAWA,[2] AND TERUHIDE YAMAGUCHI[1]*

[1]*Division of Cellular and Gene Therapy Products, National Institute of Health Sciences, Tokyo, Japan*

[2]*National Institute of Health Sciences, Tokyo, Japan*

Previously, we suggested that the phosphatidylinositol 3-kinase (PI3K)-p70 S6 kinase (p70 S6K) pathway plays an important role in granulocyte colony-stimulating factor (G-CSF)-dependent enhancement of the neutrophilic differentiation and proliferation of HL-60 cells. While atypical protein kinase C (PKC) has been reported to be a regulator of p70 S6K, abundant expression of PKCι was observed in myeloid and lymphoid cells. Therefore, we analyzed the participation of PKCι in G-CSF-dependent proliferation. The maximum stimulation of PKCι was observed from 15 to 30 min after the addition of G-CSF. From 5 to 15 min into this lag time, PKCι was found to translocate from the nucleus to the membrane. At 30 min it re-translocated to the cytosol. This dynamic translocation of PKCι was also observed in G-CSF-stimulated myeloperoxidase-positive cells differentiated from cord blood cells. Small interfering RNA for PKCι inhibited G-CSF-induced proliferation and the promotion of neutrophilic differentiation of HL-60 cells. These data indicate that the G-CSF-induced dynamic translocation and activation processes of PKCι are important to neutrophilic proliferation.

J. Cell. Physiol. 211: 189–196, 2007.

Hematopoietic cell differentiation is regulated by a complex network of growth and differentiation factors (Tenen et al., 1997; Ward et al., 2000). Granulocyte colony-stimulating factor (G-CSF) and its receptors are pivotal to the differentiation of myeloid precursors into mature granulocytes. In previous studies (Kanayasu-Toyoda et al., 2002) on the neutrophilic differentiation of HL-60 cells treated with either dimethyl sulfoxide (DMSO) or retinoic acid (RA), heterogeneous transferrin receptor (Trf-R) populations—transferrin receptor-positive ($Trf\text{-}R^+$) cells and transferrin receptor-negative ($Trf\text{-}R^-$) cells—appeared 2 days after the addition of DMSO or RA. The $Trf\text{-}R^+$ cells were proliferative-type cells that had higher enzyme activity of phosphatidylinositol 3-kinase (PI3K) and protein 70 S6 kinase (p70 S6K), whereas the $Trf\text{-}R^-$ cells were differentiation-type cells of which Tyr705 in STAT3 was much more phosphorylated by G-CSF. Inhibition of either PI3K by wortmannin or p70 S6K by rapamycin was found to eliminate the difference in differentiation and proliferation abilities between $Trf\text{-}R^+$ and $Trf\text{-}R^-$ cells in the presence of G-CSF (Kanayasu-Toyoda et al., 2002). From these results, we concluded that proteins PI3K and p70 S6K play important roles in the growth of HL-60 cells and negatively regulate neutrophilic differentiation. On the other hand, the maximum kinase activity of PI3K was observed at 5 min after the addition of G-CSF (Kanayasu-Toyoda et al., 2002) and that of p70 S6K was observed between 30 and 60 min after, indicating a lag time between PI3K and p70 S6K activation. It is conceivable that any signal molecule(s) must transduce the G-CSF signal during the time lag between PI3K and p70 S6K. Chung et al. (1994) also showed a lag time between PI3K and p70 S6K activation on HepG2 cells stimulated by platelet-derived growth factor (PDGF), suggesting that some signaling molecules also may transduce between PI3K and p70S6K.

Protein kinase C (PKC) is a family of Ser/Thr kinases involved in the signal transduction pathways that are triggered by numerous extracellular and intracellular stimuli. The PKC family has been shown to play an essential role in cellular functions, including mitogenic signaling, cytoskeleton rearrangement, glucose metabolism, differentiation, and the regulation of cell survival and apoptosis. Eleven different members of the PKC family have been identified so far. Based on their structural similarities and cofactor requirements, they have been grouped into three subfamilies: (1) the classical or conventional PKCs (cPKCα, β_1, β_2, and γ), activated by Ca^{2+}, diacylglycerol, and phosphatidyl-serine; (2) the novel PKCs (nPKCδ, ε, η, and θ), which are independent of Ca^{2+} but still responsive to diacylglycerol; and (3) the atypical PKCs (aPKCζ and ι/λ), where PKCλ is the homologue of human PKCι. Atypical PKCs differ significantly from all other PKC family

Abbreviations: DMSO, dimethyl sulfoxide; fMLP-R, formyl-Met-Leu-Phe receptor; RA, retinoic acid; G-CSF, granulocyte colony-stimulating factor; Trf-R, transferrin receptor; BSA, bovine serum albumin; FITC, fluorescein isothiocyanate; PBS, phosphate-buffered saline; PKC, protein kinase C; PI3K, phosphatidylinositol 3-kinase; p70 S6K, protein 70 S6 kinase; SDS–PAGE, sodium dodecyl sulfate-polyacrylamide gel electrophoresis; siRNA, small interfering RNA; PMN, polymorphonuclear leukocyte.

Contract grant sponsor: Ministry of Health, Labor, and Welfare of Japan.
Contract grant sponsor: Ministry of Education, Culture, Sports, Science, and Technology of Japan.

*Correspondence to: Teruhide Yamaguchi, Division of Cellular and Gene Therapy Products, National Institute of Health Sciences, 1-18-1, Kamiyoga, Setagaya-ku, Tokyo 158-8501, Japan.
E-mail: yamaguch@nihs.go.jp

Received 31 May 2006; Accepted 22 September 2006

Published online in Wiley InterScience (www.interscience.wiley.com.), 28 November 2006.
DOI: 10.1002/jcp.20930

members in their regulatory domains, in that they lack both the calcium-binding domain and one of the two zinc finger motifs required for diacylglycerol binding (Liu and Heckman, 1998). Romanelli et al. (1999) reported that p70 S6K is regulated by PKCζ and participates in a PI3K-regulated signaling complex. On the other hand, Selbie et al. (1993) reported that the tissue distribution of PKCζ is different from that of PKCι/λ, and that PKCι/λ appears to be widely expressed. If the p70 S6K could be activated by aPKC, the regulation of p70 S6K activation would seem to depend on the tissue-specific expression of PKCι and/or PKCζ. In neutrophilic lineage cells, the question is which aPKC participates in the regulation of p70 S6K on G-CSF signaling.

In this study, we show that G-CSF activated PKCι, promoting its translocation from the nucleus to the cell surface membrane and subsequently to the cytosol in DMSO-treated HL-60 cells. We also show the translocation of PKCι using myeloperoxidase-positive neutrophilic lineage differentiated from cord blood, which is a rich source of immature myeloid cells (Fritsch et al., 1993; Rappold et al., 1997; Huang et al., 1999; Debili et al., 2001; Hao et al., 2001). We concluded that PKCι translocation and activation by G-CSF are needed for neutrophilic proliferation.

Materials and Methods

Reagents

Anti-p70 S6K polyclonal antibody was obtained from Santa Cruz Biotechnology (Santa Cruz, CA). Anti-PKCι polyclonal antibody and monoclonal antibody were purchased from Santa Cruz Biotechnology and from Transduction Laboratories (Lexington, KY), respectively. Anti-PKCζ polyclonal antibody was purchased from Cell Signaling Technology (Beverly, MA). Anti-myeloperoxidase antibody was purchased from Serotec Ltd. (Oxford, UK). GF 109203X, and Gö 6983 were obtained from Calbiochem-Novabiochem (San Diego, CA). Wortmannin was obtained from Sigma Chemical (St. Louis, MO). Anti-Histon-H1 antibody, anti-Fcγ receptor IIa (CD32) antibody, and anti-lactate dehydrogenase antibody were from Upstate Cell Signaling Solutions (Lake Placid, NY), Lab Vision Corp. (Fremont, CA), and Chemicon International, Inc. (Temecula, CA), respectively.

Cell culture

HL-60, Jurkut, K562, U937, and THP-1 cells were kindly supplied by the Japanese Collection of Research Bioresources Cell Bank (Osaka, Japan). Cells were maintained in RPMI 1640 medium containing 10% heat-inactivated FBS and 30 mg/L kanamycin sulfate at 37°C in moisturized air containing 5% CO_2. The HL-60 cells, which were at a density of 2.5×10^5 cells/ml, were differentiated by 1.25% DMSO. Two days after the addition of DMSO, the G-CSF-induced signal transduction was analyzed using either magnetically sorted cells or non-sorted cells.

Magnetic cell sorting

To prepare Trf-R^- and Trf-R^+ cells, magnetic cell sorting was performed as previously reported (Kanayasu-Toyoda et al., 2002), using an automatic cell sorter (AUTO MACS; Miltenyi Biotec, Bergisch Gladbach, Germany). After cell sorting, both cell types were used for Western blotting and PKCι enzyme activity analyses.

Preparation of cell lysates and immunoblotting

For analysis of PKCι and PKCζ expression, a PVDF membrane blotted with 50 μg of various tissues per lane was purchased from BioChain Institute (Hayward, CA). Both a polymorphonuclear leukocytes (PMNs) fraction and a fraction containing lymphocytes and monocytes were isolated by centrifugation (400g, 25 min) using a Mono-poly resolving medium (Dai-Nippon Pharmaceutical, Osaka, Japan) from human whole blood, which was obtained from a healthy volunteer with informed consent. T-lymphocytes were further isolated from the mixture fraction using the Pan T Cell Isolation Kit (Miltenyi Biotec) according to the manufacturer's protocol. T-lymphocytes, PMNs, HL-60 cells, Jurkut cells, K562 cells, and U937 cells (1×10^7) were collected and lysed in lysis buffer containing 1% Triton X-100, 10 mM K_2HPO_4/KH_2PO_4 (pH 7.5), 1 mM EDTA, 5 mM EGTA, 10 mM $MgCl_2$, and 50 mM β-glycerophosphate, along with 1/100 (v/v) protease inhibitor cocktail (Sigma Chemical) and 1/100 (v/v) phosphatase inhibitor cocktail (Sigma Chemical). The cellular lysate of 10^6 cells per lane was subjected to Western blotting analysis. Human cord blood was kindly supplied from the Metro Tokyo Red Cross Cord Blood Bank (Tokyo, Japan) with informed consent. Mononuclear cells, isolated with the Lymphoprep™ Tube (Axis-Shield PoC AS, Oslo, Norway), were cultured in RPMI 1640 medium containing 10% FBS in the presence of G-CSF for 3 days. Cultured cells were collected, and the cell lysate was subjected to Western blotting analysis.

A fraction of the plasma membrane, cytosol, and nucleus of the DMSO-treated HL-60 cells was prepared by differential centrifugation after the addition of G-CSF, as described previously (Yamaguchi et al., 1999). After the cells that had been suspended in 250 mM sucrose/10 mM Tris-HCl (pH 7.4) containing 1/100 (v/v) protease inhibitor cocktail (Sigma Chemical) were gently disrupted by freezing and thawing, they were centrifuged at 800g, 4°C for 10 min. The precipitation was suspended in 10 mM Tris-HCl (pH 6.7) supplemented with 1% SDS. It was then digested by benzon nuclease at 4°C for 1 h and used as a sample of the nuclear fraction. After the post-nucleus supernatant was re-centrifuged at 100,000 rpm (452,000g) at a temperature of 4°C for 40 min, the precipitate was used as a crude membrane fraction and the supernatant as a cytosol fraction. Western blotting analysis was then performed as described previously (Kanayasu-Toyoda et al., 2002). The bands that appeared on x-ray films were scanned, and the density of each band was quantitated by Scion Image (Scion, Frederick, MD) using the data from three separate experiments.

Kinase assay

The activity of PKCι was determined by phosphorous incorporation into the fluorescence-labeled pseudosubstrate (Pierce Biotechnology, Rockford, IL). The cell lysates were prepared as described above and immunoprecipitated with the anti-PKCι antibody. Kinase activity was measured according to the manufacturer's protocol. In the analysis of inhibitors effects, cells were pretreated with a PI3K inhibitor, wortmannin (100 nM), or PKC inhibitors, GF109207X (10 μM) and Gö6983 (10 μM) for 30 min, and then stimulated by G-CSF for 15 min.

Observation of confocal laser-scanning microscopy

Upon the addition of G-CSF, PKCι localization in the DMSO-treated HL-60 cells for 2 days was examined by confocal laser-activated microscopy (LSM 510, Carl Zeiss, Oberkochen, Germany). The cells were treated with 50 ng/ml G-CSF for the indicated periods and then fixed with an equal volume of 4.0% paraformaldehyde in PBS(−). After treatment with ethanol, the fixed cells were labeled with anti-PKCι antibody and with secondary antibody conjugated with horseradish peroxidase. They were then visualized with TSA™ Fluorescence Systems (PerkinElmer, Boston, MA).

Mononuclear cells prepared from cord blood cells were cultured in RPMI 1640 medium containing 10% FBS in the presence of G-CSF for 7 days. Then, for serum and G-CSF starvation, cells were cultured in RPMI 1640 medium containing 1% BSA for 11 h. After stimulation by 50 ng/ml G-CSF, the cells were fixed, stained with both anti-PKCι polyclonal antibody and anti-myeloperoxidase monoclonal antibody, and finally visualized with rhodamine-conjugated anti-rabbit IgG and FITC-conjugated anti-mouse IgG, respectively.

RNA interference

Two pairs of siRNAs were chemically synthesized: annealed (Dharmacon RNA Technologies, Lafayette, CO) and transfected into HL-60 cells using Nucleofector™ (Amaxa, Cologne, Germany). The sequences of sense siRNAs were as follows: PKCι, GAAGAAGCCUUUAGACUUUTA; p70 S6K, GCAAGGAGUCUAUCCAUGAUU. As a control, the sequence ACUCUAUCGCCAGCGUGACUU was used. Forty-eight hours after treatment with siRNA, the cells were lysed for Western blot analysis. For proliferation and differentiation assay, cells were transfected with siRNA on the first day, treated with DMSO on the second day, and supplemented with G-CSF on the third day. After cells were subsequently cultured for 5 days, cell numbers and formyl-Met-Leu-Phe receptor (fMLP-R) expression were determined.

fMLP-R expression

The differentiated cells were collected and incubated with FITC-conjugated fMLP; then, labeled cells were subjected to flow cytometric analysis (FACSCalibur, Becton Dickinson, Franklin Lakes, NJ).

Statistical analysis

Statistical analysis was performed using unpaired Student's *t*-test. Values of $P < 0.05$ were considered to indicate statistical significance. Each experiment was repeated at least three times and representative data were indicated.

Results

The distribution of atypical PKC in various tissues and cells

Previously, we reported that the PI3K-p70 S6K-cMyc pathway plays an important role in the G-CSF-induced proliferation of DMSO-treated HL-60 cells, not only by enhancing the activity of both PI3K and p70 S6K but also by inducing the c-Myc protein (Kanayasu-Toyoda et al., 2002, 2003). We also reported that G-CSF did not stimulate Erk1, Erk2, or 4E-binding protein 1. The maximum kinase activity of PI3K was observed 5 min after the addition of G-CSF, and that of p70 S6K was observed between 30 and 60 min after. It is conceivable that any signal molecule(s) must transduce the G-CSF signal during the time lag between PI3K and p70 S6K. Romanelli et al. (1999) suggested that the activation of p70 S6K is regulated by PKCξ and participates in the PI3K-regulated signaling complex. To examine the role of atypical PKC in the G-CSF-dependent activation and the relationship between atypical PKC and p70 S6K, the protein expression of PKCζ and PKCι in various human tissues and cells was analyzed by Western blotting. As shown in Figure 1A, both of the atypical PKCs were markedly expressed in lung and kidney but were weakly expressed in spleen, stomach, and placenta. In brain, cervix, and uterus, the expression of only PKCι was observed. Selbie et al. (1993) have reported observing the expression of PKCζ not in protein levels but in RNA levels, in the kidney, brain, lung, and testis, and that of PKCι in the kidney, brain, and lung. In this study, the protein expression of PKCι in the kidney, brain, and lung was consistent with the RNA expression of PKCι. Despite the strong expression of PKCζ RNA in brain (Selbie et al., 1993), PKCζ protein was scarcely observed. Although PKCι proteins were scarcely expressed in neutrophils and T-lymphocytes in peripheral blood, they were abundantly expressed in immature blood cell lines, that is, Jurkut, K562, U937, and HL-60 cells (Fig. 1B), in contrast with the very low expression of PKCζ proteins. In mononuclear cells isolated from umbilical cord blood, which contains large numbers of immature myeloid cells and has a high proliferation ability, the expression of PKCι proteins was also observed. Since Nguyen and Dessauer (2005) have reported observing abundant PKCζ proteins in THP-1 cells, as a positive control for PKCζ, we also performed a Western blot of THP-1 cells (Fig. 1B, right part). While PKCι was markedly expressed in both THP-1 and HL-60 cells, PKCζ was observed only in THP-1 cells.

These data suggested that PKCζ and PKCι were distributed differently in various tissues and cells, and that mainly PKCι proteins were expressed in proliferating blood cells.

Stimulation of PKCι activity by G-CSF

Among the 11 different members of the PKC family, the aPKCs (ζ and ι/λ) have been reported to activate p70 S6K activity and to be regulated by PI3K (Akimoto et al., 1998; Romanelli et al., 1999). As shown in Figure 1, although the PKCζ proteins were not detected by Western blotting in HL-60 cells or mononuclear cells isolated from cord blood cells, it is possible that PKCι could functionally regulate p70 S6K as an upstream

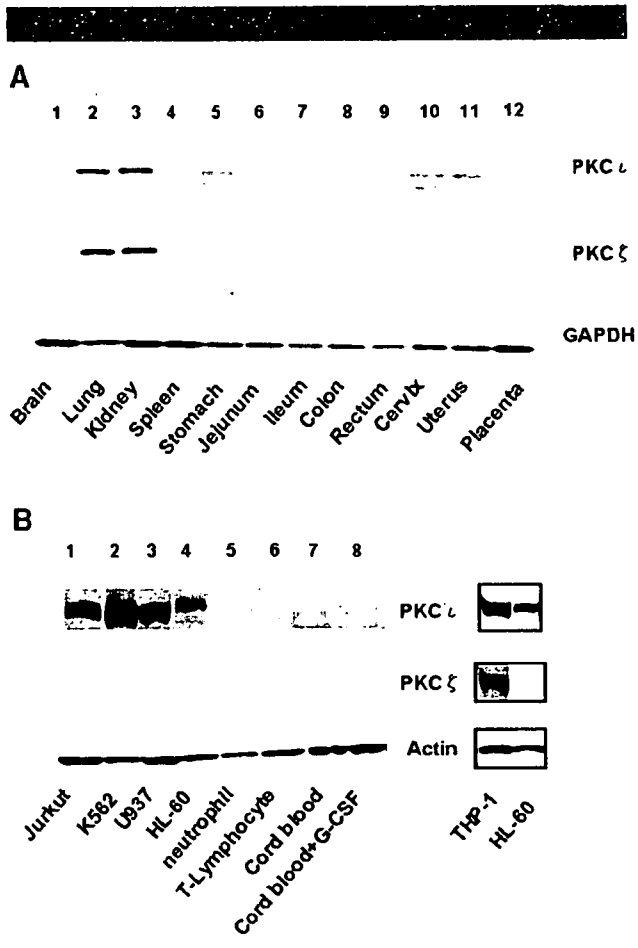

Fig. 1. Different distributions of PKCζ and PKCι. The protein expression of PKCι appears in the upper part and that of PKCζ in the middle part in various tissues and cells. A: 1, brain; 2, lung; 3, kidney, 4, spleen; 5, stomach; 6, jejunum; 7, ileum; 8, colon; 9, rectum; 10, cervix; 11, uterus; 12, placenta. Anti-GAPDH blot is a control for various tissues. B: 1, Jurkut cells; 2, K562 cells; 3, U937 cells; 4, HL-60 cells; 5, neutrophils; 6, T-lymphocytes; 7, mononuclear cells from cord blood in the absence of G-CSF; 8, mononuclear cells from cord blood in the presence of G-CSF. Anti-actin blot is a control. The right part shows immunoblots of PKCι, PKCζ, and actin of THP-1 cells as a positive control for PKCζ. The cell numbers of THP-1 and HL-60 cells were adjusted in relation to other cells on the left parts.

regulator in these cells. Therefore, we focused on the role of PKCι as the possible upstream regulator of p70 S6K in neutrophil lineage cells. First, we compared the expression of PKCι in both Trf-R^+ and Trf-R^- cells. PKCι proteins were expressed more abundantly in Trf-R^+ cells than in Trf-R^- cells (Fig. 2A, middle part), as with the p70 S6K proteins. A time course study of PKCι activity upon the addition of G-CSF revealed the maximum stimulation at 15 min, lasting until 30 min. The G-CSF-dependent activation of PKCι was inhibited by the PKC inhibitors wortmannin, GF 109203X, and Gö 6983. Considering the marked inhibitory effect of wortmannin on PKCι and evidence that the maximum stimulation of PI3K was observed at 5 min after the addition of G-CSF, PI3K was determined to be the upstream regulator of PKCι in the G-CSF signal transduction of HL-60 cells. The basal activity of PKCι in Trf-R^+ cells was higher than that in Trf-R^- cells, and G-CSF was more augmented. In Trf-R^- cells, PKCι activity was scarcely stimulated by G-CSF. This tendency of PKCι to be activated by G-CSF was similar to that of PI3K (Kanayasu-Toyoda et al., 2002).

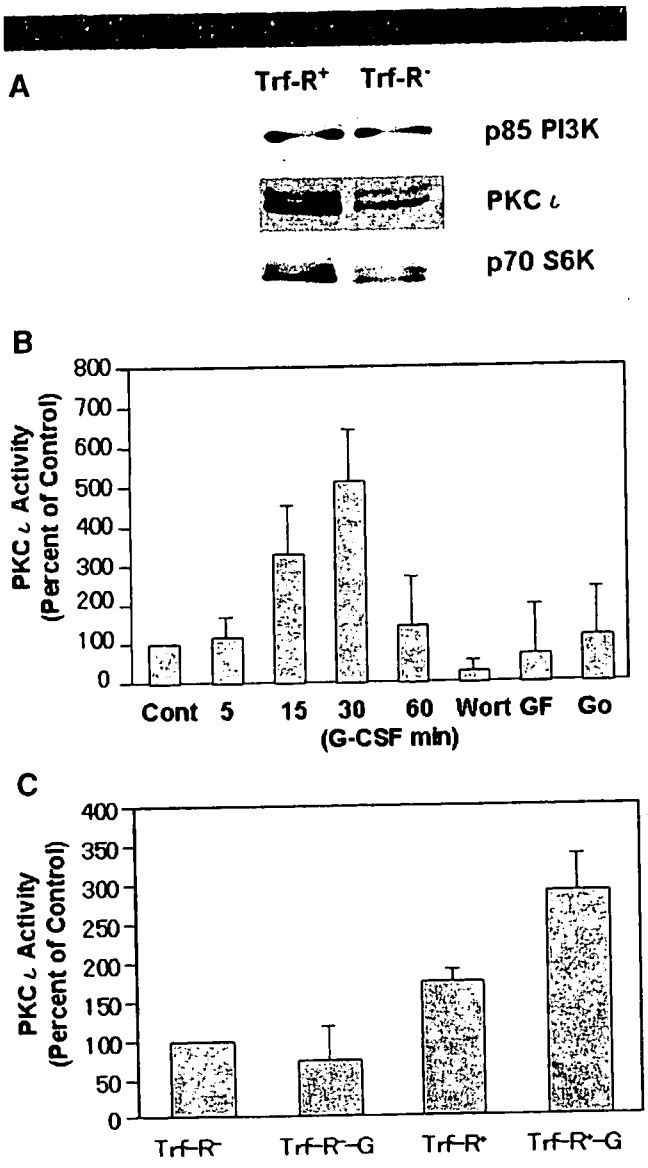

Fig. 2. Expression of PKCι in Trf-R$^+$ and Trf-R$^-$ cells and effects of G-CSF on PKCι activity. A: The expression of PKCι in Trf-R$^+$ and Trf-R$^-$ cells was subjected to Western blot analysis after magnetic cell sorting. B: The G-CSF-dependent PKCι activation of the DMSO-treated HL-60 cells was measured. The x-axis represents the time lapse (min) after the G-CSF stimulation and the y-axis percent of control that was not stimulated by G-CSF. Columns and bars represent the mean ± SD, using data from three separate experiments. Wort: wortmannin (100 nM), GF: GF109207X (10 μM), Gö: Gö6983 (10 μM). Cells were pretreated with each inhibitor and then stimulated by G-CSF for 15 min. C: The PKCι activity in the Trf-R$^+$ and Trf-R$^-$ cells 30 min after the addition of G-CSF. The y-axis represents the percentage of control that was non-stimulated Trf-R$^-$ cells. Columns and bars represent the mean ± SD, using data from three separate experiments.

Effects of G-CSF on PKCι translocation

Muscella et al. (2003) demonstrated that the translocation of PKCζ from the cytosol to the nucleus or membrane is required for c-Fos synthesis induced by angiotensin II in MCF-7 cells. It was also reported that high glucose induced the translocation of PKCι (Chuang et al., 2003). These results suggest that the translocation of aPKC plays an important role in its signaling. To clarify the translocation of PKCι, immuno-histochemical staining (Fig. 3) and biochemical fractionation (Fig. 4) in DMSO-induced HL-60 cells were performed after the addition of G-CSF. In a non-stimulated condition, PKCι in the HL-60 cells treated with DMSO for 2 days (Fig. 3, control) was detected mainly in the nucleus. Analysis of Western blotting (Fig. 4, left parts) and quantification of the bands (Fig. 4, right columns) also revealed that PKCι was localized and observed mainly in the nuclear fraction (Fig. 4A). During the 5–15 min period after the addition of G-CSF, PKCι was found to translocate (Figs. 3 and 4B) into the membrane fraction, after which it re-translocated into the cytosol fraction (Fig. 4C). In the presence of wortmannin, the G-CSF-induced translocation of PKCι into the plasma membrane failed, but PKCι was found to localize in the cytosolic fraction (Figs. 3 and 4B). Myeloperoxidase is thought to be expressed in stage from promyelocytes to mature neutrophils (Manz et al., 2002). In human cord blood cells (Fig. 3), PKCι in the cells co-stained with anti-myeloperoxidase antibody was also localized in the nucleus after serum depletion (Fig. 3B top parts). Ten minutes after the addition of G-CSF, PKCι was found to translocate into the membrane, and then into the cytosol at 30 min after the addition of G-CSF. In the presence of wortmannin, the G-CSF-induced translocation of PKCι into the plasma membrane failed but PKCι was found to localize in the cytosol. This suggested that the dynamic translocation of PKCι induced by G-CSF is a universal phenomenon in neutrophilic lineage cells. Taken together, these data support the possibility that PI3K plays not only an important role upstream of PKCι but also triggers the translocation from nucleus to membrane upon the addition of G-CSF.

In order to assess the purity of each cellular fraction, antibodies against specific markers were blotted. As specific markers, Histon-H1, Fcγ receptor IIa (CD32), and lactate dehydrogenase (LDH) were used for the nuclear, membrane, and cytosolic fractions, respectively. The purities of the nuclear, membrane, and cytosolic fractions were 82.0, 78.5, and 72.2%, respectively (Fig. 4D).

Effects of siRNA for PKCι on proliferation and differentiation

To determine the role of PKCι in neutrophilic proliferation and differentiation, PKCι was knocked down by siRNA. When the protein level of PKCι was specifically downregulated by siRNA for PKCι (Fig. 5A), G-CSF failed to enhance proliferation of the cells during 5 days' cultivation (Fig. 5B). The effect of siRNA for PKCι on neutrophilic differentiation in terms of fMLP-R expression was also determined. As shown in Figure 5C, fMLP-R expression was promoted by siRNA for PKCι in either the presence (lower part) or absence (upper part) of G-CSF. These data indicate that PKCι positively regulates G-CSF-induced proliferation and negatively regulates the differentiation of DMSO-treated HL-60 cells.

Discussion

We previously reported that PI3K/p70 S6K plays an important role in the regulation of the neutrophilic differentiation and proliferation of HL-60 cells. Akimoto et al. (1998) and Romanelli et al. (1999) reported that p70 S6K is regulated by aPKC and aPKCλ/PKCζ, respectively. At first, we showed that the distribution of PKCζ and PKCι proteins in various human tissues and cells was not similar (Fig. 1A), and that PKCι are more abundantly expressed in proliferating blood cells: Jurkut, K562, U937, and HL-60 cells (Fig. 1B). Moreover, PKCι proteins were also observed in cultured mononuclear cells of cord blood, in which the myeloid progenitors were enriched in the presence or absence of G-CSF (Fig. 1B). The myeloperoxidase-positive cells as neutrophilic lineage cells, a myeloid marker, were also stained with the antibody of PKCι (Fig. 3B). Although PKCζ proteins are barely detected in

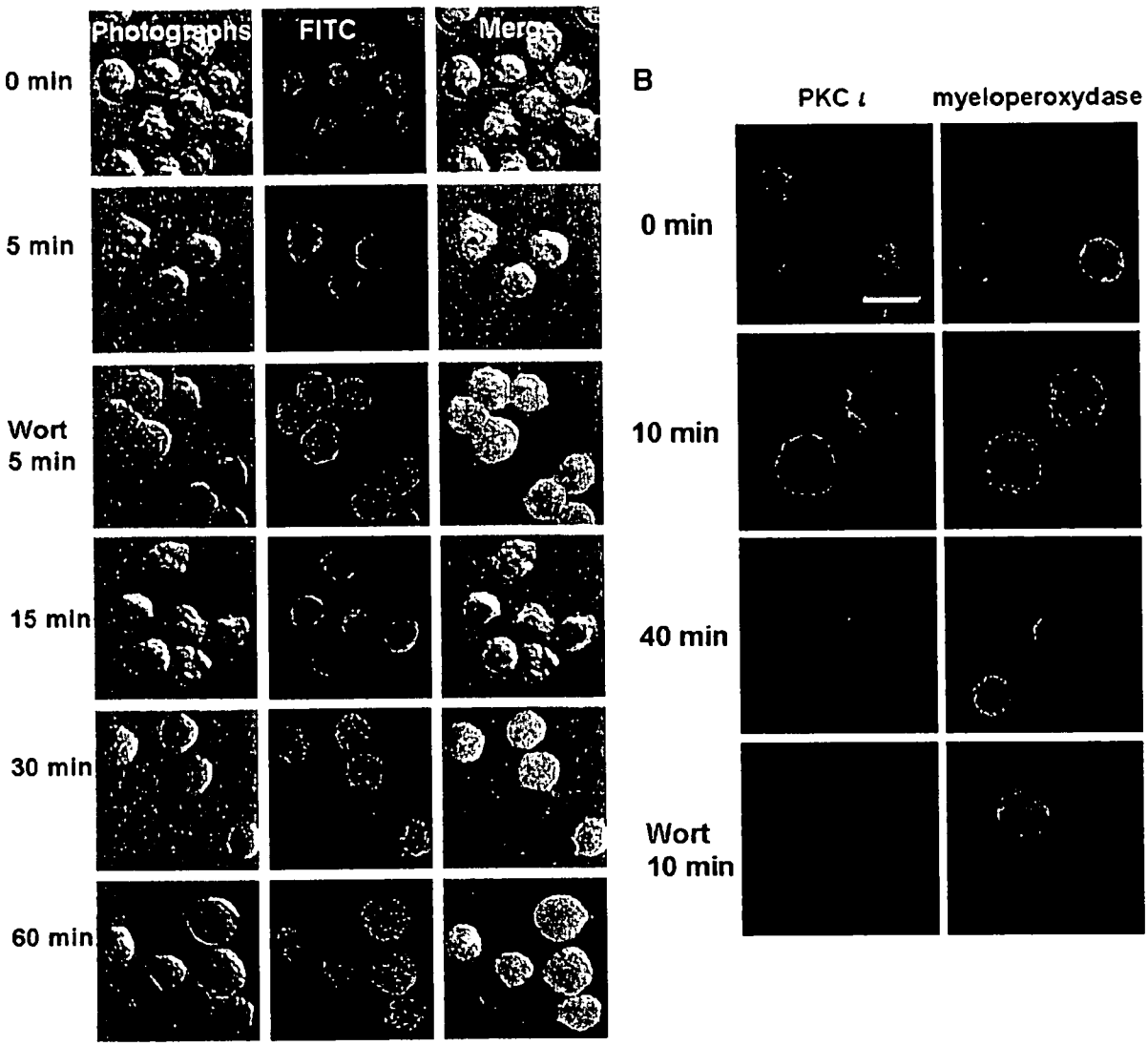

Fig. 3. Translocation of PKCι after the activation of G-CSF. A: 2 days after the addition of DMSO, HL-60 cells stimulated by G-CSF were fixed, incubated with anti-PKCι antibody, and visualized as described above. The photographs can be seen at the left part of the figure, the fluorescent photographs in the middle of the figure, and the merged images at the right. B: G-CSF-stimulated mononuclear cells from cord blood were stained with anti-PKCι antibody (red, left part) and anti-myeloperoxidase antibody (green, right part) after serum depletion. Under no stimulation, PKCι was observed in the nucleus. G-CSF promoted the translocation of PKCι to the membrane within 5–15 min, and then to the cytosol. Wort: wortmannin. White bar: 10 μm.

neutrophilic HL-60 cells, PKCι proteins were markedly expressed in these cells (Fig. 1B). This study showed, for the first time, the stimulation of PKCι activity in G-CSF-treated HL-60 cells (Fig. 2B) at 15–30 min after the addition of G-CSF. Maximum activation from the addition of NGF in PC12 cells was also observed at 15 min (Wooten et al., 2001).

Atypical PKCs are lipid-regulated kinases that need to be localized to the membrane in order to be activated. PKCζ is directly activated by phosphatidylinositol 3,4,5-trisphosphate, a product of PI3K (Nakanishi et al., 1993). We previously reported that the maximum activation of PI3K was observed in HL-60 cells 5 min after the addition of G-CSF (Kanayasu-Toyoda et al., 2002). Most investigators have reported the translocation of aPKC in either muscle cells or adipocytes stimulated by insulin (Andjelkovic et al., 1997; Goransson et al., 1998; Galetic et al., 1999; Standaert et al., 1999; Braiman et al., 2001; Chen et al., 2003; Kanzaki et al., 2004; Sasaoka et al., 2004; Herr et al., 2005). In response to insulin stimulation, aPKCζ/λ is translocated to the plasma membrane (Standaert et al., 1999; Braiman et al., 2001), where aPKCζ/λ is believed to be activated (Galetic et al., 1999; Kanzaki et al., 2004). In the present study, the addition of G-CSF induced PKCι to translocate to the membrane from the nucleus within 5–15 min (Figs. 3 and 4), and this translocation to the plasma membrane accompanied the full activation of PKCι (Fig. 2B). Previously we reported also that the maximum activation of p70 S6K in HL-60 cells was observed from 30 to 60 min after the addition of G-CSF (Kanayasu-Toyoda et al., 1999, 2002), suggesting that there was a time lag between the activation of PI3K and p70 S6K upon the addition of G-CSF in HL-60 cells. In the present study, PKCι was

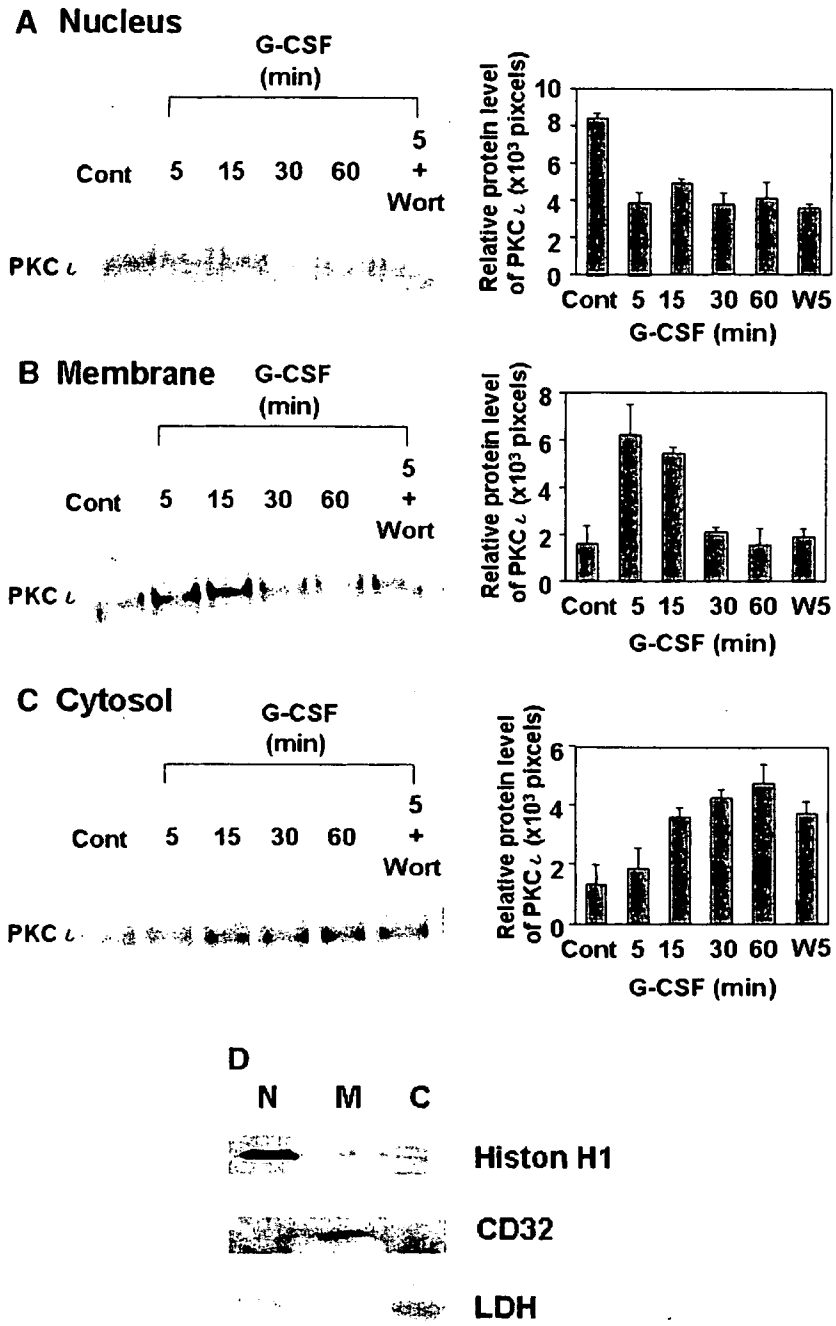

Fig. 4. Translocation of PKCι after activation by G-CSF on biochemical fractionation. The cells were differentiated as described in the Figure 3 legend. After stimulation by G-CSF, the amounts of PKCι proteins in the nucleus (A), plasma membrane (B), and cytosol (C), as fractionated by differential centrifugation, were analyzed by Western blotting (left parts). The right parts show the quantitation of the bands of PKCι proteins. Wort or W: wortmannin. PKCι protein was quantitated using data from three separate experiments. Columns and bars represent the mean ± SD. D: Each cell fraction was immunoblotted with antibodies of specific marker. Histon-H1, Fcγ receptor IIa (CD32), and lactate dehydrogenase (LDH) are specific markers for nuclear (N), membrane (M), and cytosolic (C) fractions, respectively.

found to re-translocate from the plasma membrane to the cytosol (Figs. 3 and 4C). In the presence of wortmannin, an inhibitor of PI3K, PKCι failed to translocate into the plasma membrane, but instead translocated to cytosol directly from the nucleus upon the addition of G-CSF (Figs. 3 and 4B). PKCι translocation was also observed in myeloperoxidase-positive cells derived from human cord blood (Fig. 3B), indicating that G-CSF-induced dynamic translocation of PKCι occurred in not only a limited cell line but also neutrophilic lineage cells. These data suggest that PI3K plays an important role in the activation and translocation of PKCι during the G-CSF-induced activation of myeloid cells. Furthermore, the translocation to the plasma membrane in response to G-CSF is wortmannin sensitive, but the translocation from the nucleus upon G-CSF stimulation is not affected by wortmannin, suggesting that the initial signal of G-CSF-induced PKCι translocation from the nucleus may be

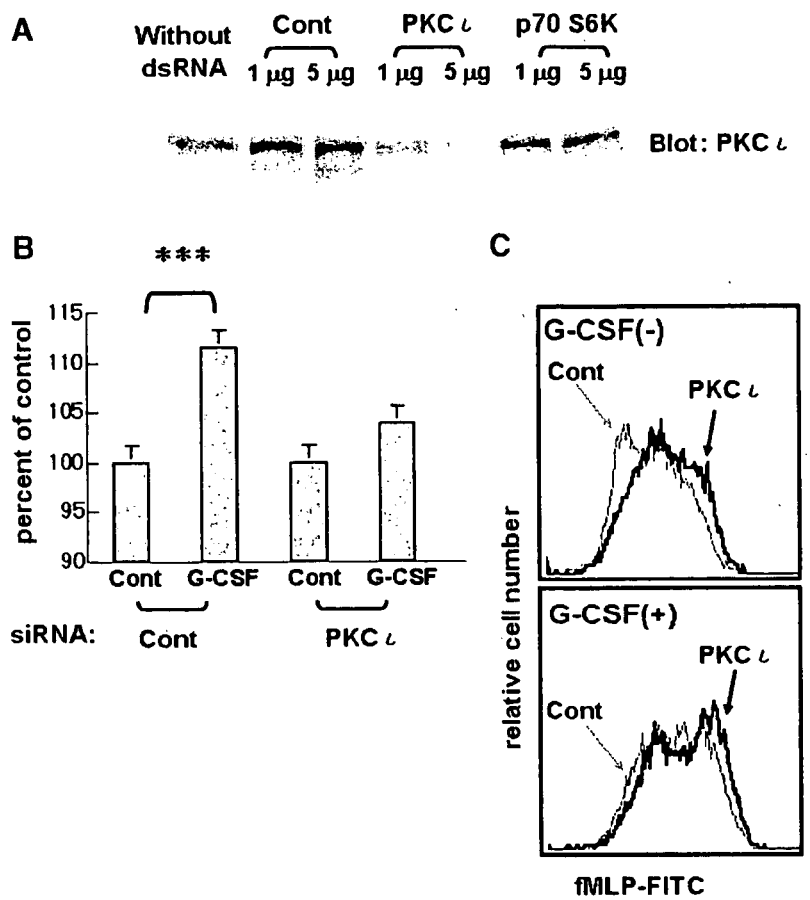

Fig. 5. Effects of siRNA of PKCι on proliferation, differentiation, and phosphorylation at various sites of p70 S6K. A: Forty-eight hours after transfection with siRNA of PKCι or p70 S6K, protein levels of PKCι were compared. B: Proliferation of the cells transfected with siRNA of PKCι or control (Cont) was measured 5 days after the addition of G-CSF. Columns and bars represent the mean ± SD of triplicate wells (*$P < 0.001$). C: fMLP-R expression was analyzed by flow cytometry 5 days after the addition of G-CSF. The gray arrow indicates cells transfected with the control sequence of double-stranded RNA (Cont, gray lines), and the black arrow the cells transfected with siRNA for PKCι (black lines) in the presence (lower part) or absence (upper part) of G-CSF.**

PI3K-independent, but association of PKCι with the plasma membrane could be mediated through a PI3K-dependent signal. Cord blood is an important material of blood transplantation for leukemia (Bradstock et al., 2006; Ooi, 2006; Yamada et al., 2006) or for congenital neutropenia (Mino et al., 2004; Nakazawa et al., 2004) because it contains many hematopoietic stem cells such as CD34-positive cells or CD133-positive cells, and also contains immature granulocytes. The neutrophilic differentiation and proliferation are necessary processes after transplantation.

Formyl-Met-Leu-Phe peptide evokes the migration, superoxide production, and phagocytosis of neutrophils through fMLP-R, a suitable marker for neutrophilic differentiation. In this study, the reduction of PKCι by siRNA inhibited G-CSF-induced proliferation (Fig. 5B) and promoted neutrophilic differentiation (Fig. 5C) in terms of fMLP-R expression. These data, however, suggest that PKCι promoted G-CSF-induced proliferation and blocked differentiation at the same time.

The substrates of aPKC have recently been reported: namely, the cytoskeletal protein Lethal giant larvae (Lgl) was phosphorylated by Drosophila aPKC (Betschinger et al., 2003) and glyceraldehydes-3-phosphate dehydrogenase (GAPDH) was phosphorylated by PKCι (Tisdale, 2002) directly in both cases. While the direct phosphorylation of p70 S6K by aPKC was not observed (Akimoto et al., 1998; Romanelli et al., 1999), the enzyme activity of p70 S6K was markedly enhanced by co-transfection with aPKC and PDK-1, the latter of which is recruited to the membrane due to the binding of phosphatidylinositol-3,4,5-trisphosphate to its PH domain (Anderson et al., 1998). The addition of G-CSF induced PKCι to increase phosphorylation at Thr-389, which is the site most closely related to enzyme activity among the multi-phosphorylation sites of p70 S6K (Weng et al., 1998). However, the mammalian target of rapamycin (mTOR), an upstream regulator, also phosphorylates Thr-389 of p70 S6K and markedly stimulates p70 S6K activity under coexistence with PDK-1 (Isotani et al., 1999). We could not rule out the possibility that other PKC isoforms can contribute to the activation of p70 S6K. We postulated that in G-CSF-stimulated HL-60 cells, PKCι contributes to p70 S6K activation as an upstream regulator.

Atypical PKC isoforms are reported to play an important role in the activation of IκB kinase β (Lallena et al., 1999). In PKCζ-deficient mice, impaired signaling through the B-cell receptor resulted in the inhibition of cell proliferation and survival while also causing defects in the activation of ERK and the transcription of NF-κB-dependent genes (Martin et al., 2002). Moreover, Lafuente et al. (2003) demonstrated that the loss of Par-4, that is, the genetic inactivation of the aPKC inhibitor, led to an increased proliferative response of

peripheral T cells when challenged through the T-cell receptor. However, it has been reported that PKCλ-deficient mice have a lethal phenotype at the early embryonic stage (Soloff et al., 2004). Based on the present results and those of previous reports (Kanayasu-Toyoda et al., 1999, 2002), we postulate that PKCι plays an important role in regulating G-CSF-induced proliferation in neutrophilic lineage cells.

Acknowledgments

We thank the Metro Tokyo Red Cross Cord Blood Bank (Tokyo, Japan) for their kind cooperation. This work was supported in part by a grand-in-aid for health and labor science research (H17-SAISEI-021) from the Japanese Ministry of Health, Labor and Welfare, and in part by a grand-in-aid for Research on Health Sciences focusing on Drug Innovation from the Japan Health Sciences Foundation.

Literature Cited

Akimoto K, Nakaya M, Yamanaka T, Tanaka J, Matsuda S, Weng QP, Avruch J, Ohno S. 1998. Atypical protein kinase Clambda binds and regulates p70 S6 kinase. Biochem J 335:417–424.

Anderson KE, Coadwell J, Stephens LR, Hawkins PT. 1998. Translocation of PDK-1 to the plasma membrane is important in allowing PDK-1 to activate protein kinase B. Curr Biol 8:684–691.

Andjelkovic M, Alessi DR, Meier R, Fernandez A, Lamb NJ, Frech M, Cron P, Cohen P, Lucocq JM, Hemmings BA. 1997. Role of translocation in the activation and function of protein kinase B. J Biol Chem 272:31515–31524.

Betschinger J, Mechtler K, Knoblich JA. 2003. The Par complex directs asymmetric cell division by phosphorylating the cytoskeletal protein Lgl. Nature 422:326–330.

Bradstock KF, Hertzberg MS, Kerridge IH, Svennilson J, McGurgan M, Huang G, Antonenas V, Gottlieb DJ. 2006. Unrelated umbilical cord blood transplantation for adults with haematological malignancies: Results from a single Australian centre. Intern Med J 36:355–361.

Braiman L, Alt A, Kuroki T, Ohba M, Bak A, Tennenbaum T, Sampson SR. 2001. Activation of protein kinase C zeta induces serine phosphorylation of VAMP2 in the GLUT4 compartment and increases glucose transport in skeletal muscle. Mol Cell Biol 21:7852–7861.

Chen X, Al-Hasani H, Olausson T, Wenthzel AM, Smith U, Cushman SW. 2003. Activity, phosphorylation state and subcellular distribution of GLUT4-targeted Akt2 in rat adipose cells. J Cell Sci 116:3511–3518.

Chuang LY, Guh JY, Liu SF, Hung MY, Liao TN, Chiang TA, Huang JS, Huang YL, Lin CF, Yang YL. 2003. Regulation of type II transforming-growth-factor-beta receptors by protein kinase C iota. Biochem J 375:385–393.

Chung J, Grammer TC, Lemon KP, Kazlauskas A, Blenis J. 1994. PDGF- and insulin-dependent p70 S6K activation mediated by phosphatidylinositol-3-OH kinase. Nature 370:71–75.

Debili N, Robin C, Schiavon V, Letestu R, Pflumio F, Mitjavila-Garcia MT, Coulombel L, Vainchenker W. 2001. Different expression of CD41 on human lymphoid and myeloid progenitors from adults and neonates. Blood 97:2023–2030.

Fritsch G, Buchinger P, Printz D, Fink FM, Mann G, Peters C, Wagner T, Adler A, Gadner H. 1993. Rapid discrimination of early CD34+ myeloid progenitors using CD45-RA analysis. Blood 81:2301–2309.

Galetic I, Andjelkovic M, Meier R, Brodbeck D, Park J, Hemmings BA. 1999. Mechanism of protein kinase B activation by insulin/insulin-like growth factor-1 revealed by specific inhibitors of phosphoinositide 3-kinase—Significance for diabetes and cancer. Pharmacol Ther 82:409–425.

Goransson O, Wijkander J, Manganiello V, Degerman E. 1998. Insulin-induced translocation of protein kinase B to the plasma membrane in rat adipocytes. Biochem Biophys Res Commun 246:249–254.

Hao QL, Zhu J, Price MA, Payne KJ, Barsky LW, Crooks GM. 2001. Identification of a novel, human multilymphoid progenitor in cord blood. Blood 97:3683–3690.

Herr HJ, Bernard JR, Reeder DW, Rivas DA, Limon JJ, Yaspelkis BB3rd. 2005. Insulin-stimulated plasma membrane association and activation of Akt2, aPKC zeta and aPKC lambda in high fat fed rodent skeletal muscle. J Physiol 565:627–636.

Huang S, Chen Z, Yu JF, Young D, Bashey A, Ho AD, Law P. 1999. Correlation between IL-3 receptor expression and growth potential of human CD34+ hematopoietic cells from different tissues. Stem Cells 17:265–272.

Isotani S, Hara K, Tokunaga C, Inoue H, Avruch J, Yonezawa K. 1999. Immunopurified mammalian target of rapamycin phosphorylates and activates p70 S6 kinase alpha in vitro. J Biol Chem 274:34493–34498.

Kanayasu-Toyoda T, Yamaguchi T, Uchida E, Hayakawa T. 1999. Commitment of neutrophilic differentiation and proliferation of HL-60 cells coincides with expression of transferrin receptor. Effect of granulocyte colony stimulating factor on differentiation and proliferation. J Biol Chem 274:25471–25480.

Kanayasu-Toyoda T, Yamaguchi T, Oshizawa T, Kogi M, Uchida E, Hayakawa T. 2002. Role of the p70 S6 kinase cascade in neutrophilic differentiation and proliferation of HL-60 cells—a study of transferrin receptor-positive and -negative cells obtained from dimethyl sulfoxide- or retinoic acid-treated HL-60 cells. Arch Biochem Biophys 405:21–31.

Kanayasu-Toyoda T, Yamaguchi T, Oshizawa T, Uchida E, Hayakawa T. 2003. The role of c-Myc on granulocyte colony-stimulating factor-dependent neutrophilic proliferation and differentiation of HL-60 cells. Biochem Pharmacol 66:133–140.

Kanzaki M, Mora S, Hwang JB, Saltiel AR, Pessin JE. 2004. Atypical protein kinase C (PKCzeta/lambda) is a convergent downstream target of the insulin-stimulated phosphatidylinositol 3-kinase and TC10 signaling pathways. J Cell Biol 164:279–290.

Lafuente MJ, Martin P, Garcia-Cao I, Diaz-Meco MT, Serrano M, Moscat J. 2003. Regulation of mature T lymphocyte proliferation and differentiation by Par-4. Embo J 22:4689–4698.

Lallena MJ, Diaz-Meco MT, Bren G, Paya CV, Moscat J. 1999. Activation of IkappaB kinase beta by protein kinase C isoforms. Mol Cell Biol 19:2180–2188.

Liu WS, Heckman CA. 1998. The sevenfold way of PKC regulation. Cell Signal 10:529–542.

Manz MG, Miyamoto T, Akashi K, Weissman IL. 2002. Prospective isolation of human clonogenic common myeloid progenitors. Proc Natl Acad Sci USA 99:11872–11877.

Martin P, Duran A, Minguet S, Gaspar ML, Diaz-Meco MT, Rennert P, Leitges M, Moscat J. 2002. Role of zeta PKC in B-cell signaling and function. Embo J 21:4049–4057.

Mino E, Kobayashi R, Yoshida M, Suzuki Y, Yamada M, Kobayashi K. 2004. Umbilical cord blood stem cell transplantation from unrelated HLA-matched donor in an infant with severe congenital neutropenia. Bone Marrow Transplant 33:969–971.

Muscella A, Greco S, Elia MG, Storelli C, Marsigliante S. 2003. PKC-zeta is required for angiotensin II-induced activation of ERK and synthesis of C-FOS in MCF-7 cells. J Cell Physiol 197:61–68.

Nakanishi H, Brewer KA, Exton JH. 1993. Activation of the zeta isozyme of protein kinase C by phosphatidylinositol 3,4,5-trisphosphate. J Biol Chem 268:13–16.

Nakazawa Y, Sakashita K, Kinoshita M, Saida K, Shigemura T, Yanagisawa R, Shikama N, Kamijo T, Koike K. 2004. Successful unrelated cord blood transplantation using a reduced-intensity conditioning regimen in a 6-month-old infant with congenital neutropenia complicated by severe pneumonia. Int J Hematol 80:287–290.

Nguyen BT, Dessauer CW. 2005. Relaxin stimulates protein kinase C zeta translocation: Requirement for cyclic adenosine 3',5'-monophosphate production. Mol Endocrinol 19:1012–1023.

Ooi J. 2006. The efficacy of unrelated cord blood transplantation for adult myelodysplastic syndrome. Leuk Lymphoma 47:599–602.

Rappold I, Ziegler BL, Kohler I, Marchetto S, Rosnet O, Birnbaum D, Simmons PJ, Zannettino AC, Hill B, Neu S, Knapp W, Alitalo R, Alitalo K, Ullrich A, Kanz L, Buhring HJ. 1997. Functional and phenotypic characterization of cord blood and bone marrow subsets expressing FLT3 (CD135) receptor tyrosine kinase. Blood 90:111–125.

Romanelli A, Martin KA, Toker A, Blenis J. 1999. p70 S6 kinase is regulated by protein kinase Czeta and participates in a phosphoinositide 3-kinase-regulated signalling complex. Mol Cell Biol 19:2921–2928.

Sasaoka T, Wada T, Fukui K, Murakami S, Ishihara H, Suzuki R, Tobe K, Kadowaki T, Kobayashi M. 2004. SH2-containing inositol phosphatase 2 predominantly regulates Akt2, and not Akt1, phosphorylation at the plasma membrane in response to insulin in 3T3-L1 adipocytes. J Biol Chem 279:14835–14843.

Selbie LA, Schmitz-Peiffer C, Sheng Y, Biden TJ. 1993. Molecular cloning and characterization of PKC iota, an atypical isoform of protein kinase C derived from insulin-secreting cells. J Biol Chem 268:24296–24302.

Soloff RS, Katayama C, Lin MY, Feramisco JR, Hedrick SM. 2004. Targeted deletion of protein kinase C lambda reveals a distribution of functions between the two atypical protein kinase C isoforms. J Immunol 173:3250–3260.

Standaert ML, Bandyopadhyay G, Perez L, Price D, Galloway L, Poklepovic A, Sajan MP, Cenni V, Sirri A, Moscat J, Toker A, Farese RV. 1999. Insulin activates protein kinases C-zeta and C-lambda by an autophosphorylation-dependent mechanism and stimulates their translocation to GLUT4 vesicles and other membrane fractions in rat adipocytes. J Biol Chem 274:25308–25316.

Tenen DG, Hromas R, Licht JD, Zhang DE. 1997. Transcription factors, normal myeloid development, and leukemia. Blood 90:489–519.

Tisdale EJ. 2002. Glyceraldehyde-3-phosphate dehydrogenase is phosphorylated by protein kinase Ciota/lambda and plays a role in microtubule dynamics in the early secretory pathway. J Biol Chem 277:3334–3341.

Ward AC, Loeb DM, Soede-Bobok AA, Touw IP, Friedman AD. 2000. Regulation of granulopoiesis by transcription factors and cytokine signals. Leukemia 14:973–990.

Weng QP, Kozlowski M, Belham C, Zhang A, Comb MJ, Avruch J. 1998. Regulation of the p70 S6 kinase by phosphorylation in vivo. Analysis using site-specific anti-phosphopeptide antibodies. J Biol Chem 273:16621–16629.

Wooten MW, Vandenplas ML, Seibenhener ML, Geetha T, Diaz-Meco MT. 2001. Nerve growth factor stimulates multisite tyrosine phosphorylation and activation of the atypical protein kinase C's via a src kinase pathway. Mol Cell Biol 21:8414–8427.

Yamada K, Mizusawa M, Harima A, Kajiwara K, Hamaki T, Hoshi K, Kozai Y, Kodo H. 2006. Induction of remission of relapsed acute myeloid leukemia after unrelated donor cord blood transplantation by concomitant low-dose cytarabine and calcitriol in adults. Eur J Haematol 77:345–348.

Yamaguchi T, Mukasa T, Uchida E, Kanayasu-Toyoda T, Hayakawa T. 1999. The role of STAT3 in granulocyte colony-stimulating factor-induced enhancement of neutrophilic differentiation of Me2SO-treated HL-60 cells. GM-CSF inhibits the nuclear translocation of tyrosine-phosphorylated STAT3. J Biol Chem 274:15575–15581.

Available online at www.sciencedirect.com
ScienceDirect
Journal of Chromatography A, 1160 (2007) 263–269
JOURNAL OF CHROMATOGRAPHY A
www.elsevier.com/locate/chroma

Study on the quality control of cell therapy products Determination of *N*-glycolylneuraminic acid incorporated into human cells by nano-flow liquid chromatography/Fourier transformation ion cyclotron mass spectrometry

Noritaka Hashii [a,b], Nana Kawasaki [a,b,*], Yukari Nakajima [a,b], Masashi Toyoda [c], Yoko Katagiri [c], Satsuki Itoh [a], Akira Harazono [a], Akihiro Umezawa [c], Teruhide Yamaguchi [a]

[a] *Division of Biological Chemistry and Biologicals, National Institute of Health Sciences, 1-18-1 Kamiyouga, Setagaya-ku, Tokyo 158-8501, Japan*
[b] *Core Research for Evolutional Science and Technology (CREST) of Japan Science and Technology Agency (JST), 4-1-8 Hon-cho, Kawaguchi, Saitama 332-0012, Japan*
[c] *National Research Institute for Child Health and Development, 2-10-1 Okura, Setagaya-ku, Tokyo 157-8535, Japan*

Received 6 February 2007; received in revised form 16 May 2007; accepted 21 May 2007
Available online 25 May 2007

Abstract

N-Glycolylneuraminic acid (NeuGc), an acidic nine-carbon sugar, is produced in several animals, such as cattle and mice. Since human cells cannot synthesize NeuGc, it is considered to be immunogenic in humans. Recently, NeuGc contamination was reported in human embryonic stem cells cultured with xenogeneic serum and cells, suggesting that possibly NeuGc may harm the efficacy and safety of cell therapy products. Sialic acids have been determined by derivatization with 1,2-diamino-4,5-methylenedioxybenzene (DMB) followed by liquid chromatography/mass spectrometry (LC/MS) and liquid chromatography/tandem mass spectrometry (LC/MS/MS); however, the limited availability of cell therapy products requires more sensitive and specific methods for the quality test. Here we studied the use of nano-flow liquid chromatography/Fourier transformation ion cyclotron resonance mass spectrometry (nanoLC/FTMS) and nanoLC/MS/MS for NeuGc-specific determination at a low femtomole level. Using our method, we found NeuGc contamination of the human cell line (HL-60RG cells) cultured with human serum. Our method needs only 2.5×10^3 cells for one injection and would be applicable to the determination of NeuGc in cell therapy products.

Keywords: *N*-Glycolylneuraminic acid; Nano-flow liquid chromatography; Fourier transformation ion cyclotron mass spectrometry; Cell therapy products

1. Introduction

Sialic acids are a family of acidic nine-carbon sugars found in the non-reducing terminal of *N*-linked and *O*-linked oligosaccharides of glycoproteins and glycolipids [1,2]. There are more than 30 members with different substitutions on the amino group at carbon 5 and on hydroxyl groups at carbons 4, 7, 8 and 9 [2–8]. *N*-Glycolylneuraminic acid (NeuGc), a 5-*N*-glycolylated sialic acid, is produced in several animals, such as cattle, horses, mice and rats [9]. Since human cells cannot synthesize NeuGc due to mutation of the cytidine monophospho (CMP)-*N*-acetylneuraminic acid (NeuAc) hydroxylase gene [10,11], NeuGc is considered to be antigenic and to induce immunoreaction in humans [4,12,13].

Advances in biotechnology and cell culture techniques make it possible to administer human and animal cells directly to patients as cell therapy products. In cell therapy and tissue engineering, human embryonic stem (ES) cells are expected to be useful for the treatment of many diseases. Recently, it was reported that NeuGc is incorporated into ES cells from human and mouse feeder cells and cultivation media containing xenogeneic serum, such as fetal calf serum (FCS) [14,15]. Since NeuGc is a foreign component in humans, it is feared that NeuGc may harm the efficacy and safety of cell therapy products. To

* Corresponding author. Tel.: +81 3 3700 9074; fax: +81 3 3700 9084.
E-mail address: nana@nihs.go.jp (N. Kawasaki).

0021-9673/$ – see front matter © 2007 Elsevier B.V. All rights reserved.
doi:10.1016/j.chroma.2007.05.062

assess the adverse effects of NeuGc, it is necessary to quantify NeuGc in cell therapy products.

Sialic acids have been determined by labeling with 1,2-diamino-4,5-methylenedioxybenzene (DMB) followed by conventional high-performance liquid chromatography (HPLC) with fluorescent detection [16–20]. The femtomole level of sialic acid can be determined by fluorescent detection [19]. The use of liquid chromatography/mass spectrometry (LC/MS) and liquid chromatography/tandem mass spectrometry (LC/MS/MS) has more advantage in the identification of sialic acid species [18,20–22]. The derivatization of sialic acids with DMB has advantages of good separation of NeuGc from NeuAc in chromatography and enhancement of ionization efficiency in MS. However, more sensitive and specific methods are desired for the quality control of cell therapy products, since in many case only a low number of cell products, approximately 1×10^6 to 1×10^8, should be available for quality tests.

In this study, we studied the use of nano-flow liquid chromatography/Fourier transformation ion cyclotron resonance mass spectrometry (nanoLC/FTMS) and LC/MS/MS to achieve the sensitive and specific determination of NeuGc. The potential of the method for quality testing of cell therapy products was evaluated using substrain of human promyelocytic leukemia HL-60 cells (HL-60RG cells) as model cells. Using this method, we determined NeuGc in membrane fractions from HL-60RG cells cultured with FCS, human serum and serum-free medium.

2. Experimental

2.1. Materials

NeuGc and NeuAc were purchased from Nacalai Tesque (Kyoto, Japan). FCS and normal human serum were purchased from Dainippon Sumitomo Pharma (Osaka, Japan). RPMI1640 medium and ASF104 medium were purchased from Sigma-Aldrich (St. Louis, MO, USA) and Ajinomoto (Tokyo, Japan), respectively.

2.2. Cell culture

Substrain of human promyelocytic leukemia HL-60 cells (HL-60RG cells, JCRB Cellbank, Osaka, Japan) was cultured in RPMI1640 medium supplemented with 10% FCS, 100 unit/ml of penicillin and 100 μg/ml of streptomycin under a humidified atmosphere of 95% air and 5% CO_2 at 37 °C. HL-60RG cells were replaced at 2×10^5 cells/100 mm dish in RPMI1640 medium supplemented with 10% FCS or 10% normal human serum, and in serum-free ASF104 medium. The media were replaced four times, and semi-confluent growth cells were harvested.

2.3. Fractionation of the membrane fraction

The cells were washed in phosphate buffer saline (PBS) supplemented with protease inhibitors (protease inhibitor mix solution, Wako, Tokyo, Japan) three times. The washed cells (1×10^6) were suspended in 100 μl of 0.25 M sucrose/10 mM Tris–HCl buffer (pH 7.4) containing protease inhibitors, and sonicated at 4 °C for 30 s, two times (40W, Bioruptor UCW-201, Tosyoudenki, Kanagawa, Japan). After the nuclei were removed by centrifugation at 4 °C, 450 × *g* for 10 min, the mitochondria and lysosome fractions were removed by re-centrifugation at 4 °C, 20,000 × *g* for 10 min. The membrane fractions were precipitated by ultracentrifugation at 4 °C, 100,000 × *g* for 60 min. The membrane fractions were washed in 100 μl of 150 mM ammonium acetate buffer (pH 7.4) and recovered by re-ultracentrifugation.

2.4. Derivatization of NeuGc and NeuAc with DMB reagent

The membrane fractions were sonicated in 250 μl of H_2O and then incubated with 250 μl of 4 M acetic acid (final concentration, 2 M) at 80 °C for 3 h. The released sialic acids were passed though a solid-phase extraction cartridge (SepPak C-18, Waters, Milford, MA, USA) with 2 ml of H_2O, dried under vacuum, and resolved in 50 μl of H_2O. The solution was incubated with DMB according to the manufacturer's instruction (Takara, Tokyo, Japan), and the reaction mixture was applied on a solid-phase extraction cartridge (Envi-Carb C, Supelco, Bellefonte, PA, USA). After washing the cartridge with 2.5 ml of 5 mM ammonium acetate (pH 9.6) for desalting, the DMB-labeled sialic acids were eluted with 3 ml of 45% acetonitrile/5 mM ammonium acetate (pH 9.6). The collected fraction was freeze dried.

2.5. nanoLC/FTMS

DMB-labeled sialic acids were separated by HPLC using Paradigm MS4 (Michrom BioResource, Auburn, CA, USA) equipped with a reversed-phase C18 column (Magic C18, 50 mm × 0.1 mm, 3 μm, Michrom BioResource, Auburn, CA, USA). Elution was achieved using 0.1% formic acid/2% ace-

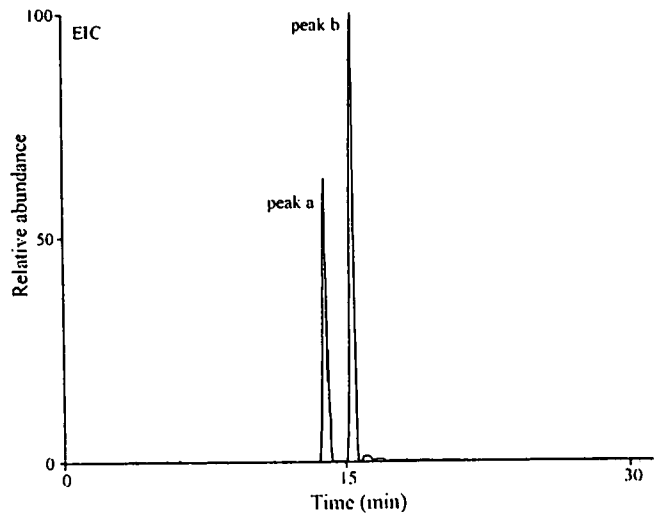

Fig. 1. EIC at *m/z* 426.13–426.17 and *m/z* 442.12–442.16 obtained by SIM (*m/z* 400–450) of DMB-NeuGc and DMB-NeuAc in the positive ion mode.

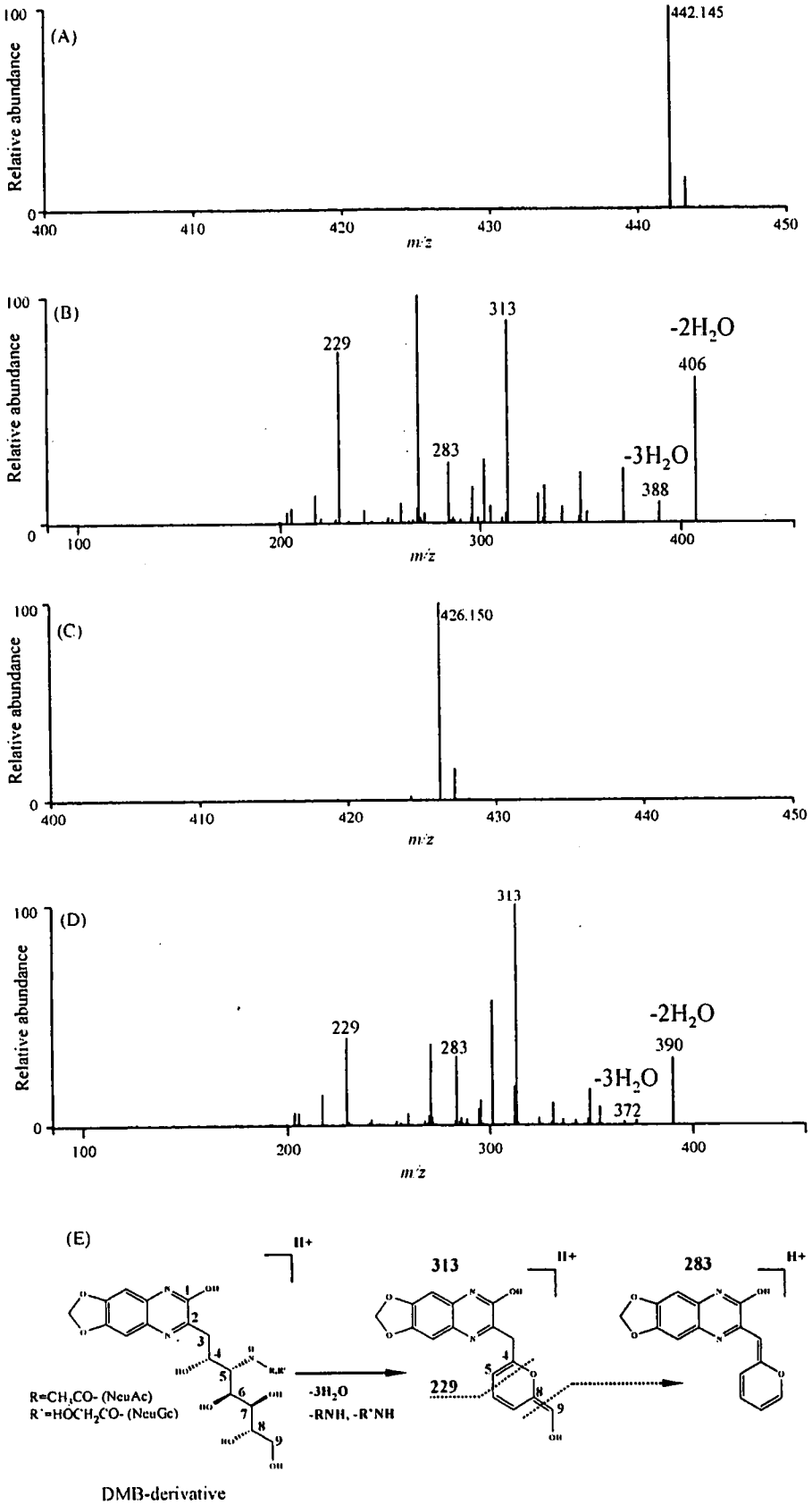

Fig. 2. (A) Typical MS spectrum of peak a. (B) MS/MS spectrum of $[M+H]^+$ (*m/z* 442.145) acquired from around peak a. (C) Typical MS spectrum of peak b. (D) MS/MS spectrum of $[M+H]^+$ (*m/z* 426.150) acquired from around peak b. (E) Fragmentation of DMB-NeuGc and DMB-NeuAc.

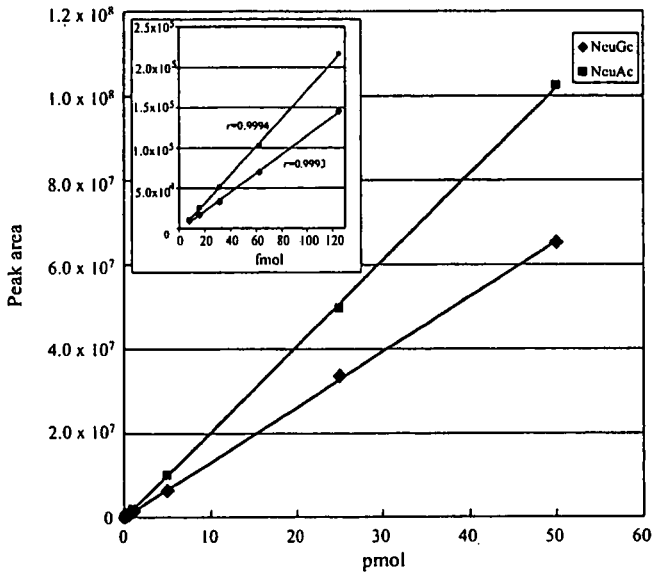

Fig. 3. Calibration curves of DMB-NeuGc ($r = 0.9998$) and DMB-NeuAc ($r = 0.9995$).

tonitrile (pump A) and 0.1% formic acid/80% acetonitrile (pump B) with a linear gradient of 10–90% of B in 30 min at a flow rate of 750 nl/min. On-line MS and MS/MS were performed using an Fourier transformation ion cyclotron resonance (FT)/ion trap (IT) type mass spectrometer (LTQ-FT, Thermo-Electron, San Jose, CA, USA) equipped with a nanoelectrospray ion source (AMR, Tokyo, Japan). DMB-NeuAc and DMB-NeuGc were determined by selected ion monitoring (SIM) in the positive ion mode. The analytical conditions were set to 200 °C for capillary temperature, 1800 eV spray voltage, *m/z* 400–450 scan range, and 35% collision energy. The automatic gain control (AGC) value, which is adjusted for the amount of imported ions for FTMS, was set to 5×10^4. Maximum injection times, which are the adjusted times of imported ions, for ITMS and FTMS, were set to 50 and 1250 ms, respectively.

2.6. Method validation

The linearity of the signal intensity peak area of DMB-NeuAc and DMB-NeuGc was assessed by injections of 0.0078–500 pmol DMB derivatives. Correlation coefficients were calibrated using a least-squares linear regression model. The detection limit (DL) and the quantification limit (QL) were calculated using the formulas DL = 3.3 × σ/slope (σ: average of noise on chromatograph) and QL = 10 × σ/slope, respectively. Accuracy and precision were determined by measuring three samples, where NeuGc spiked at the concentration of 50 fmol to the membrane fraction of cells cultured in serum-free medium which contains no NeuGc before the derivatization of NeuGc with DMB. Accuracy was calculated by comparison of the mean peak area and the calibration curve. Precision was estimated by relative standard deviation (RSD) from three samples.

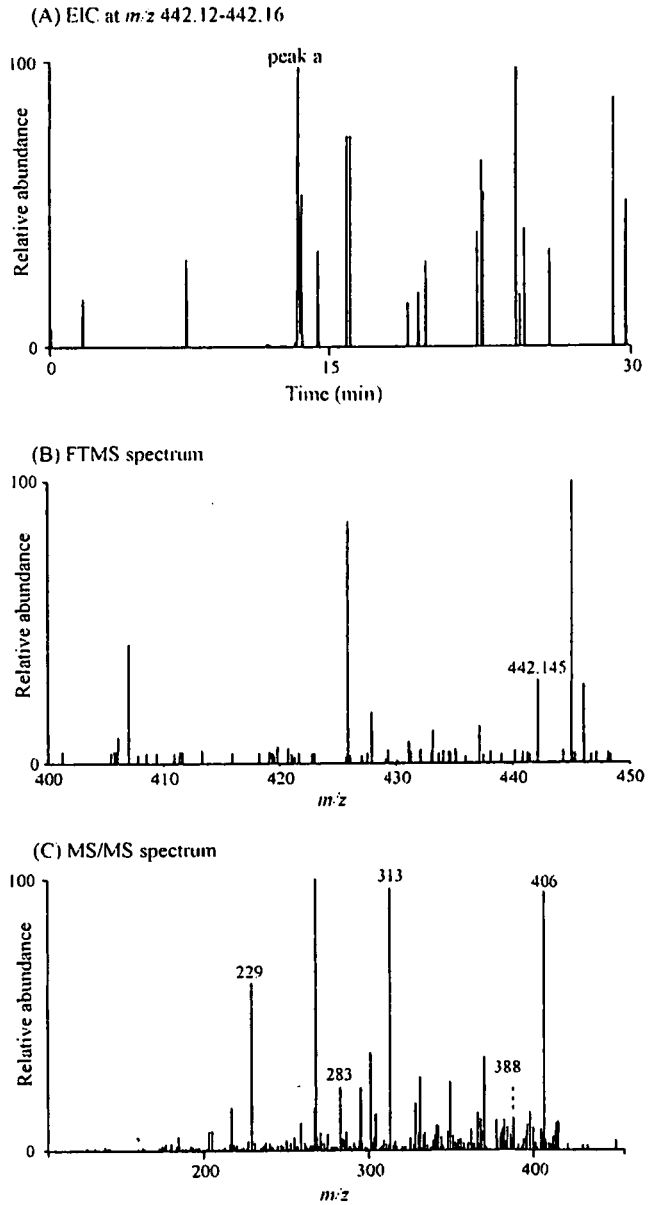

Fig. 4. Detection of DMB-NeuGc in the membrane fractions of HL-60RG cells (2.5×10^3) cultured with 10% FCS. (A) EIC at *m/z* 442.12–442.16 obtained by SIM. (B) Typical MS spectrum of peak a. (C) MS/MS spectrum of $[M+H]^+$ (*m/z* 442.145) acquired from around peak a.

3. Results and discussion

3.1. Analysis of NeuGc and NeuAc by nanoLC/FTMS

It was reported that DMB-NeuGc yielded its dehydrated ion (*m/z* 424) together with molecular ion (*m/z* 442) by MS in the positive ion mode [18,21]. To control the dehydration of molecular ion in the ion trap device, AGC value, which regulates the amount of ions trapped into ion trap device, was set to 5×10^4 (default value, 5×10^5). This value was also useful for the detection of molecular ion of DMB-NeuAc.

Using the AGC value at 5×10^4, SIM (*m/z* 400–450) was carried out in the positive ion mode. When a mix-

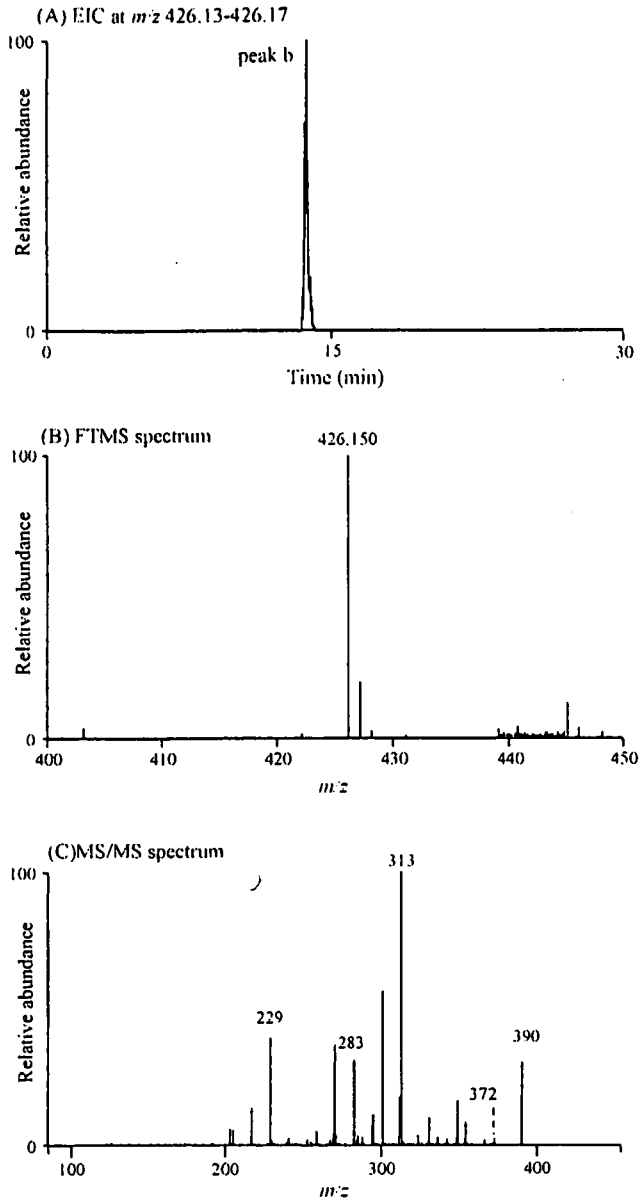

Fig. 5. Detection of DMB-NeuAc in the membrane fractions of HL-60RG cells (2.5×10^3) cultured with 10% FCS. (A) EIC at *m/z* 426.13–426.17 obtained by SIM. (B) Typical MS spectrum of peak b, (C) MS/MS spectrum of $[M+H]^+$ (*m/z* 426.150) acquired from around peak b.

ture of DMB-NeuGc and DMB-NeuAc (2 pmol each) was subjected to nanoLC/MS, two peaks appeared at 14 min (peak a) and 15 min (peak b) on the extracted ion chromatogram (EIC) at *m/z* 426.13–426.17 and *m/z* 442.12–442.16 (Fig. 1).

As shown in Fig. 2A, the *m/z* values of molecular ions around 14 min (*m/z* 442.145) suggest the elution of DMB-NeuGc in peak a. The structure of the DMB derivative at peak a was confirmed by the product ion spectra acquired from $[M+H]^+$ (*m/z* 442.145) as a precursor ion (Fig. 2B). Product ions missing two and three molecules of H_2O were found at *m/z* 406 and 388 in MS/MS spectra. Ions losing three H_2O and glycolyl groups (*m/z* 313), cross-ring fragment ion (*m/z* 229) and fragment ion yielded by loss of formaldehyde (*m/z* 283) were also formed by

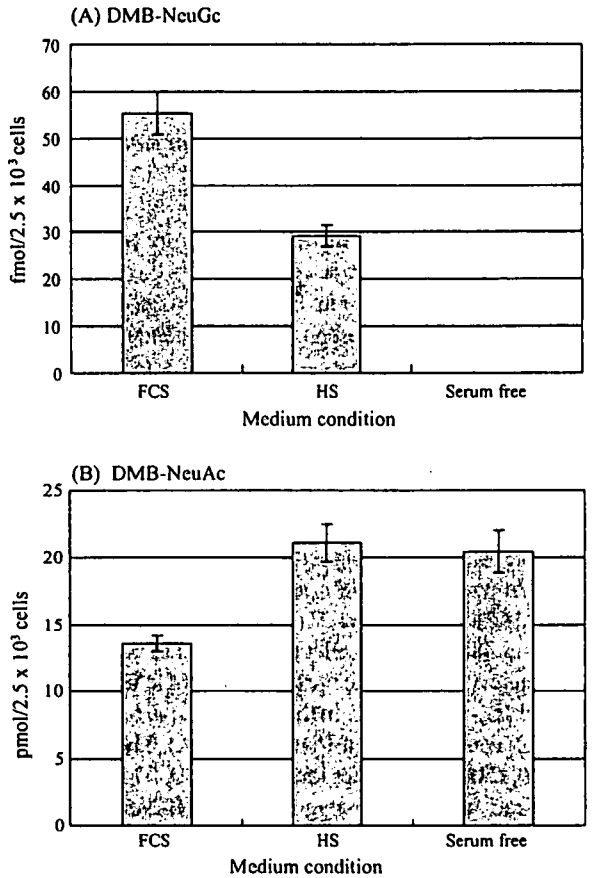

Fig. 6. Levels of (A) NeuGc and (B) NeuAc in the membrane fraction of HL-60RG cells (2.5×10^3) cultured with 10% FCS, 10% human serum (HS) and serum-free medium. Values are the means ± SD ($n = 3$).

MS/MS (Fig. 2E). The fragment pattern of the MS/MS spectrum from $[M+H]^+$ (*m/z* 442.145) was consistent with that of DMB-NeuGc in the previous report [21]. Fragments at *m/z* 406 and 388 are DMB-NeuGc characteristic ions, which could be used for specific determination of DMB-NeuGc. Likewise, peak b was identified as DMB-NeuAc by molecular ions (*m/z* 426.150) and their product ions (*m/z* 390, 372, 313, 283 and 229) formed by MS/MS of $[M+H]^+$ (*m/z* 426.150) as a precursor ion (Fig. 2C and D).

Calibration curves were prepared by the injection of DMB-NeuGc and DMB-NeuAc from 0.0078 to 500 pmol. The linearity of DMB-NeuGc and DMB-NeuAc was confirmed in the range of 0.0078–50 pmol with the regression equations of $Y = 1.31 \times 10^6 X - 9028.5$ ($r = 0.9998$) and $Y = 2.03 \times 10^6 X - 21548.0$ ($r = 0.9995$), respectively (Fig. 3). DL and QL of DMB-NeuGc were 8.6 and 26.3 fmol, and those of DMB-NeuAc were 5.6 and 16.9 fmol, respectively. The use of FT/MS gave an accuracy of 92.4% by eliminating contaminants by using accurate *m/z* values. The precision of this method for NeuGc was 7.3%. Compared to the former method, in which a micro or semi-micro column and the quadrupole mass spectrometer were used for the detection of picomole levels of DMB derivatives, SIM by using nanoLC/FTMS achieved the specific detection of DMB-derivatized sialic acids at a lower level. The method using nanoLC/FTMS and nanoLC/MS/MS allows not

only the determination of DMB-derivatives with similar sensitivity as the fluorescence detection but also the identification of sialic acid species.

3.2. Quantification of NeuAc and NeuGc in membrane fraction of HL-60RG cells

Using HL-60RG cells as model cells, the potential of this method for the quantification of NeuGc on the cell membrane was evaluated. The membrane fraction from cells (1×10^6) cultured with 10% FCS was prepared by ultracentrifugation. Sialic acids were released by treatment with 2 M acetic acid at 80 °C for 3 h and derivatized with DMB. DMB derivatives (2.5×10^3 cells) were subjected to nanoLC/MS and nanoLC/MS/MS in SIM mode. As shown in Fig. 4A, some peaks appeared in EIC at *m/z* 442.12–442.16. Based on the retention time as well as the *m/z* value of molecular ion (*m/z* 442.145), peak a that appeared at 14 min was assigned to be a peak of NeuGc (Fig. 4B). Fig. 4C shows the MS/MS spectrum acquired from $[M+H]^+$ (*m/z* 442.145) as precursor. The NeuGc-characteristic ions at *m/z* 406 and 388 together with other product ions at *m/z* 313, 283 and 229 clearly indicate the presence of NeuGc in the membrane fraction of HL-60RG cells. In the EIC at *m/z* 426.13–426.17, the single peak was observed at 15 min (Fig. 5A). The molecular ion at *m/z* 426.150, and product ions at *m/z* 390, 372, 313, 283 and 229 acquired at 15.13 min suggest that DMB-NeuAc is eluted in peak b (Fig. 5B and C). The levels of NeuGc and NeuAc in the membrane fraction from HL-60RG cells (2.5×10^3 cells) cultured with 10% FCS were 55.4 ± 4.6 fmol and 13.5 ± 0.6 pmol, respectively (Fig. 6)

After the cultivation of HL-60RG cells with human serum for 10 days (medium was changed four times), NeuGc and NeuAc were determined by the proposed method. Fig. 7A shows the EIC at *m/z* 442.12–442.16 obtained by nanoLC/MS. In spite of cultivation in human serum, an obvious peak still appeared at 14 min. Molecular ion (*m/z* 442.145) and NeuGc-characteristic product ions found in the MS/MS spectrum acquired from the molecular ion clearly indicate the presence of NeuGc in the membrane fraction (Fig. 7B and C). The levels of NeuGc and NeuAc in cells (2.5×10^3) cultured in 10% human serum were 29.2 ± 2.4 fmol and 21.0 ± 1.4 pmol, respectively (Fig. 6).

In contrast, no significant peaks appeared in EIC at *m/z* 442.12–442.16 when HL-60RG cells were cultured in serum-free medium for 14 days (medium was changed four times). The level of NeuAc in cells cultured in serum-free medium was 20.5 ± 1.6 pmol (Fig. 6).

As shown in Figs. 4A and 7A, there are many different molecules detected at *m/z* 442.14–442.16 in the cells, which makes it difficult to determine a small amount of NeuGc in the membrane fraction by the low-resolution mass spectrometry. The DMB-NeuGc-specific detection was achieved by acquisition of both the accurate mass by FTMS and the characteristic product ions arisen from DMB-NeuGc by MS/MS.

Our method needs only 2.5×10^3 cells for one injection and is applicable to the determination of NeuGc in cell therapy products. The incorporation of dietary NeuGc into human serum has been reported by Tangvoranuntalul et al. [23], which has raised concerns about NeuGc contamination of cell therapy products through cultivation with human serum. Although using our method, we demonstrated the existence of NeuGc in human cells cultured with human serum, NeuGc could not be detected in human cells cultured in serum-free medium in which no NeuGc exists. These results suggest the difficulty of avoiding NeuGc contamination of cell therapy products during the manufacturing process. Further study to assess the immunogenicity of incorporated NeuGc is necessary to ensure the safety and efficacy of cell therapy products, and our method is useful for the sensitive and quantitative analysis of NeuGc in cell therapy products.

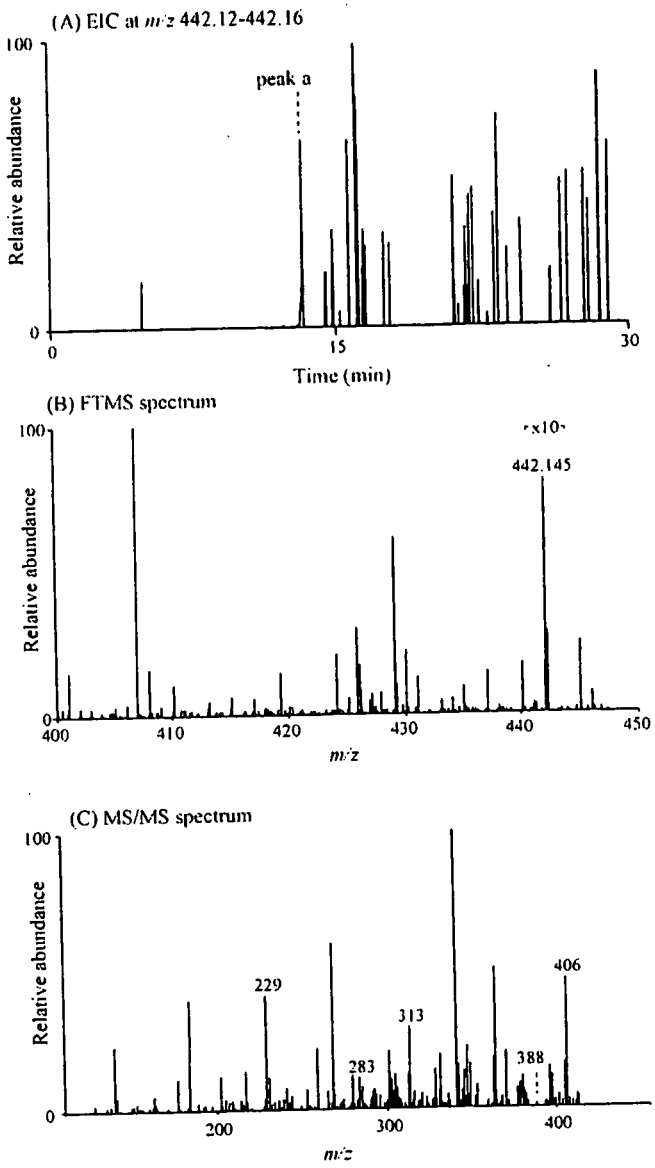

Fig. 7. Detection of DMB-NeuGc in the membrane fractions of HL-60RG cells (2.5×10^3) cultured with 10% human serum. (A) EIC at *m/z* 442.12–442.16 obtained by SIM. (B) Typical MS spectrum of peak a. (C) MS/MS spectrum of $[M+H]^+$ (*m/z* 442.145) acquired from around peak a.

Acknowledgements

This study was supported in part by a Grant-in-Aid from the Ministry of Health Labor and Welfare, and Core Research for the Evolutional Science and Technology Program, Japan Science and Technology Corp.

References

[1] C. Traving, R. Schauer, Cell Mol. Life Sci. 54 (1998) 1330.
[2] T. Angata, A. Varki, Chem. Rev. 102 (2002) 439.
[3] A. Varki, Glycobiology 2 (1992) 25.
[4] R. Schauer, Adv. Carbohydr. Chem. Biochem. 40 (1982) 131.
[5] S. Kitazume, K. Kitajima, S. Inoue, S.M. Haslam, H.R. Morris, A. Dell, W.J. Lennarz, Y. Inoue, J. Biol. Chem. 271 (1996) 6694.
[6] R. Schauer, J. Haverkamp, M. Wember, J.P. Kamerling, J.F. Vliegenthart, Eur. J. Biochem. 62 (1976) 237.
[7] N. Kawasaki, S. Itoh, M. Ohta, T. Hayakawa, Anal. Biochem. 316 (2003) 15.
[8] M. Nakano, K. Kakehi, M.H. Tsai, Y.C. Lee, Glycobiology 14 (2004) 431.
[9] E.A. Muchmore, S. Diaz, A. Varki, Am. J. Phys. Anthropol. 107 (1998) 187.
[10] A. Irie, S. Koyama, Y. Kozutsumi, T. Kawasaki, A. Suzuki, J. Biol. Chem. 273 (1998) 15866.
[11] H.H. Chou, H. Takematsu, S. Diaz, J. Iber, E. Nickerson, K.L. Wright, E.A. Muchmore, D.L. Nelson, S.T. Warren, A. Varki, Proc. Natl. Acad. Sci. U. S. A. 95 (1998) 11751.
[12] H. Higashi, M. Naiki, S. Matuo, K. Okouchi, Biochem. Biophys. Res. Commun. 79 (1977) 388.
[13] J.M. Merrick, K. Zadarlik, F. Milgrom, Int. Arch. Allergy Appl. Immunol. 57 (1978) 477.
[14] M.J. Martin, A. Muotri, F. Gage, A. Varki, Nat. Med. 11 (2005) 228.
[15] A. Heiskanen, T. Satomaa, S. Tiitinen, A. Laitinen, S. Mannelin, U. Impola, M. Mikkola, C. Olsson, H. Miller-Podraza, M. Blomqvist, A. Olonen, H. Salo, P. Lehenkari, T. Tuuri, T. Otonkoski, J. Natunen, J. Saarinen, J. Laine, Stem Cells 25 (2007) 197.
[16] A.E. Manzi, S. Diaz, A. Varki, Anal. Biochem. 188 (1990) 20.
[17] S. Hara, M. Yamaguchi, Y. Takemori, K. Furuhata, H. Ogura, M. Nakamura, Anal. Biochem. 179 (1989) 162.
[18] M. Bardor, D.H. Nguyen, S. Diaz, A. Varki, J. Biol. Chem. 280 (2005) 4228.
[19] M. Ito, K. Ikeda, Y. Suzuki, K. Tanaka, M. Saito, Anal. Biochem. 300 (2002) 260.
[20] F.N. Lamari, N.K. Karamanos, J. Chromatogr. B 781 (2002) 3.
[21] A. Klein, S. Diaz, I. Ferreira, G. Lamblin, P. Roussel, A.E. Manzi, Glycobiology 7 (1997) 421.
[22] H.H. Chou, T. Hayakawa, S. Diaz, M. Krings, E. Indriati, M. Leakey, S. Paabo, Y. Satta, N. Takahata, A. Varki, Proc. Natl. Acad. Sci. U. S. A. 99 (2002) 11736.
[23] P. Tangvoranuntakul, P. Gagneux, S. Diaz, M. Bardor, N. Varki, A. Varki, E. Muchmore, Proc. Natl. Acad. Sci. U. S. A. 100 (2003) 12045.